

SoRoSim: a MATLAB[®] Toolbox for Soft Robotics Based on the Geometric Variable-strain Approach

Anup Teejo Mathew¹, Ikhlas Ben Hmida¹, Costanza Armanini¹, Frederic Boyer², Federico Renda^{*1,3},

Abstract

Soft robotics has been a trending topic within the robotics community for almost two decades. However, the available tools for the community to model and analyze soft robotics artifacts are still limited. This paper presents the development of a user-friendly MATLAB[®] toolbox, SoRoSim, that integrates the Geometric Variable Strain model to facilitate the modeling, analysis, and simulation of hybrid rigid-soft open-chain robotic systems. The toolbox implements a recursive, two-level nested quadrature scheme to solve the model. We demonstrate several examples and applications to validate the toolbox and explore the toolbox's capabilities to efficiently model a vast range of robotic systems, considering different actuators and external loads, including the fluid-structure interactions. We think that the soft-robotics research community will benefit from the SoRoSim toolbox for a wide variety of applications.

Keywords: Soft Robot Modeling, Continuum Manipulators, Flexible Manipulators, MATLAB Toolbox.

1. Introduction

One of the most trending topics in the robotics community during the last years is the development of soft materials to design robots that can tackle some challenges that are otherwise hard to solve using their traditional, rigid counterparts.¹ Soft robots are cheap, light, and easily adaptable to different environments and scenarios, as demonstrated by the vast number of application fields where they have been employed. On the other side, their compliance and infinite number of degrees of freedom (DoF) intrinsically increase the complexity of their theoretical modelling. Different modelling approaches have been proposed, varying in their simplifying assumptions and applicability.²⁻⁴ The development of theoretical solutions that provide precise modelling capabilities is indeed crucial, but theory alone may not be enough to satisfy the demand for computational

tools in the robotics field. Knowledge-sharing initiatives are crucial to allow the growth of a relatively new research field such as soft robotics.⁵

Some examples of such initiatives have been introduced in recent years, including SoMo,⁶ a python-based program that can be used to simulate continuum manipulators as approximated spring-mass systems. On the other end, SOFA, a simulation tool that initially focused mostly on medical applications, employs a simplified Finite Element approach that has been applied to the modelling and control of soft robots.^{7,8} Another tool recently proposed in the robotics community is Elastica,⁹ which employs Discrete Geometry and the Cosserat rod theory to model and control dynamic slender bodies with a finite number of lumped degrees of freedom. Another tool namely, VIPER¹⁰ uses a Volume Invariant Position-based Elastic Rods model to sim-

* Corresponding author federico.renda@ku.ac.ae

¹ Department of Mechanical Engineering, Khalifa University of Science and Technology, Abu Dhabi, UAE.

² LS2N Laboratory, Institut Mines Telecom Atlantique, Nantes 44307, France

³ Khalifa University Center for Autonomous Robotic Systems (KUCARS), Khalifa University, Abu Dhabi, UAE.

ulate the behaviour of muscular hydrostats. Finally, the MATLAB package, TMTDyn by Sadiati et al.,¹¹ which uses discretized lumped systems and reduced-order models, is also an example in this direction. However, the majority of the available software for soft robotics modeling uses a theoretically simple but computationally heavy approach, with a lot of nodes and DOFs, designed for a general purpose simulation, instead of analysis and control. Within this scenario, we present the SoRoSim, which is a MATLAB toolbox based on the geometrically exact variable strain (GVS) approach.^{12,13} The approach directly extends the rigid robot modeling to soft and hybrid systems and bridges their gap. It allows the modelling, simulation, analysis, and control of rigid, soft and hybrid open-chain structures within the same framework. Moreover, as a MATLAB toolbox, it can be used together with other MATLAB addons such as the Optimization Toolbox¹⁴ and the Control System Toolbox¹⁵ to further facilitate the analysis and control process.

We summarize the GVS model and present a new, explicit approach to solve the Lagrangian matrices of the dynamic equation. The new approach consists of a two-level nested quadrature scheme (Gaussian quadrature and Zanna collocation) and recursive formulas to compute all quantities of the equation.

The paper is organised as follows. Section 2 provides some background on the GVS approach that represents the foundation of the proposed toolbox, while section 3 introduces the new computational approach. Section 4 details the toolbox structure and serves as a user manual to define the robot components, the actuation, and external forces and solve static and dynamic problems using the toolbox. In Section 5, the toolbox is validated by comparing with a numerical test result from a previous work and by analyzing the energy balance of a dynamic soft system, while in Section 6 a vast number of application examples is proposed. Finally, in Section 7 some conclusions and future prospects are drawn.

2. The Geometric Variable-strain Approach

The Geometric Variable-strain (GVS) approach was introduced by Renda et al.¹² in statics and Boyer et al.¹³ in dynamics. It is based

on a strain parametrization of the soft links represented by Cosserat rods. It is geometrically-exact and generalizes the geometric theory of rigid robotics¹⁶ to hybrid systems of soft and rigid links with multidimensional joints and distributed actuation forces.¹⁷

In Boyer et al.,¹³ the authors use an implicit method based on a reduced Newton–Euler (NE) inverse dynamic algorithm to calculate the Lagrangian matrices of the dynamic equation. Contrary, an explicit approach is proposed here based on a recursive computation of the kinematic Jacobian and its time derivative. In the following, the kinematics and dynamics of the GVS model are presented in an explicit form that reflects this computational choice. After that, the Constant-strain (CS) case, which is preparatory for our computational implementation, is analyzed.

2.1. Kinematics

A floating hybrid kinematic chain is composed of interconnected rigid and soft bodies, here represented by Cosserat rods. The configuration of a soft body i (respectively a rigid body) with respect to its predecessor in the chain is defined as a curve

$$\begin{aligned} \mathbf{g}_i(\cdot) : X_i \in [0, L_i] &\mapsto \\ \mathbf{g}_i(X_i) = \begin{pmatrix} \mathbf{R}_i & \mathbf{r}_i \\ \mathbf{0} & 1 \end{pmatrix} &\in SE(3). \end{aligned} \quad (1)$$

(respectively a point $\mathbf{g}_i \in SE(3)$), mapping the body-frame at X_i to the body-frame of the previous body at the reference configuration, as shown in Figure 1.

[Figure 1 about here.]

To study the exponential representation of (1), we introduce its partial derivatives with respect to space (indicated by $(\cdot)'$) and time (indicated by (\cdot)). We obtain

$$\begin{aligned} \mathbf{g}'_i(X_i) &= \mathbf{g}_i \widehat{\boldsymbol{\xi}}_i, \\ \dot{\mathbf{g}}_i(X_i) &= \mathbf{g}_i \widehat{\boldsymbol{\eta}}_i^r, \end{aligned} \quad (2)$$

where

$$\begin{aligned} \widehat{\boldsymbol{\xi}}_i(X_i) &= \begin{pmatrix} \tilde{\mathbf{k}}_i & \mathbf{p}_i \\ \mathbf{0} & 0 \end{pmatrix} \in \mathfrak{se}(3), \\ \boldsymbol{\xi}_i(X_i) &= (\mathbf{k}_i^T, \mathbf{p}_i^T)^T \in \mathbb{R}^6, \end{aligned} \quad (3)$$

defines the strain twist in body-frame, and

$$\begin{aligned}\widehat{\boldsymbol{\eta}}_i^r(X_i) &= \begin{pmatrix} \tilde{\mathbf{w}}_i^r & \mathbf{v}_i^r \\ \mathbf{0} & 0 \end{pmatrix} \in \mathfrak{se}(3), \\ \boldsymbol{\eta}_i^r(X_i) &= (\mathbf{w}_i^{rT}, \mathbf{v}_i^{rT})^T \in \mathbb{R}^6,\end{aligned}\quad (4)$$

is the velocity twist relative to the predecessor in body-frame. In (3), $\tilde{\mathbf{k}}_i(X) \in \mathfrak{so}(3)$, $\mathbf{k}_i(X) \in \mathbb{R}^3$ and $\mathbf{p}_i(X) \in \mathbb{R}^3$ are, respectively, the angular and linear strains. In (4), $\tilde{\mathbf{w}}_i^r(X) \in \mathfrak{so}(3)$, $\mathbf{w}_i^r(X) \in \mathbb{R}^3$ and $\mathbf{v}_i^r(X) \in \mathbb{R}^3$ are, respectively, the angular and linear velocity relative to the predecessor.

To develop the Product of Exponentials (PoE) formula as the forward kinematics of the hybrid-chain, we first notice that equation (2) holds for both, rigid and soft bodies, thanks to the following analogy. Imagine labeling the configuration of a rigid link i with a continuous independent variable $X_i \in [0, 1]$ where $X_i = 0$ refers to the "initial" configuration, $X_i = 1$ points to the link body-frame "after" the joint motion, and the rest indicates the intermediate poses. Thanks to this analogy, the "initial" ($X_i = 0$) configuration of the rigid link corresponds to the Cosserat rod's base, while the "final" ($X_i = 1$) pose corresponds to the rod's tip. Clearly, we are interested only in the "final" ($X_i = 1$) configuration in the rigid body case, since the other frames are immaterial.

Now, the first of the equations in (2) is a matrix differential equation that can be integrated in space. For the rigid link case, $\widehat{\boldsymbol{\xi}}_i(X_i)$ is constant in X_i and equal to the body-frame representation of the joint twist attached to i , while for the soft link case, $\widehat{\boldsymbol{\xi}}_i(X_i)$ is variable. Thus, the integration provides respectively:

$$\mathbf{g}_i(1) = \exp\left(\widehat{\boldsymbol{\xi}}_i\right), \quad (5)$$

$$\mathbf{g}_i(L_i) = \exp\left(\widehat{\boldsymbol{\Omega}}_i(L_i)\right) \quad (6)$$

(note that $\mathbf{g}_i(0) = \mathbf{I}$), where $\widehat{\boldsymbol{\Omega}}_i(L_i)$ is the Magnus expansion¹⁸ of $\widehat{\boldsymbol{\xi}}_i$ at $X_i = L_i$, an integral series of Lie Brackets of $\widehat{\boldsymbol{\xi}}_i(X_i)$. The exponential map in $SE(3)$ ¹⁹ is provided in Appendix 7. Finally, the configuration of a link i with respect to the spatial frame can be obtained via a PoE formula.

$$\begin{aligned}\mathbf{g}_{si}(X_i) &= \mathbf{g}_{s0} \exp\left(\widehat{\boldsymbol{\xi}}_0\right) \mathbf{g}_{01} \exp\left(\widehat{\boldsymbol{\xi}}_1 \text{ or } \widehat{\boldsymbol{\Omega}}_1(L_1)\right) \\ &\dots \exp\left(\widehat{\boldsymbol{\Omega}}_i(X_i)\right),\end{aligned}\quad (7)$$

where $\widehat{\boldsymbol{\xi}}_0$ parametrizes the floating frame of the root body, and \mathbf{g}_{ij} is the fixed rigid body transformation between two consecutive links in the reference configuration (see Figure 1). The forward kinematics (7) maps the strain twists $\widehat{\boldsymbol{\xi}}_i(X_i)$ to the pose of any link in the hybrid chain, provided that the Magnus expansion $\widehat{\boldsymbol{\Omega}}_i(X_i)$ can be computed. Such computation is given in section 3.

Next, we seek to find a relation between the time derivative of the strain twists and the links velocity and acceleration twists. Considering the equality of the mixed partial derivative of \mathbf{g}_i , we obtain²⁰

$$\boldsymbol{\eta}_i^{r'}(X_i) = \dot{\boldsymbol{\xi}}_i - \text{ad}_{\boldsymbol{\xi}_i} \boldsymbol{\eta}_i^r, \quad (8)$$

$$\dot{\boldsymbol{\eta}}_i^{r''}(X_i) = \ddot{\boldsymbol{\xi}}_i - \text{ad}_{\dot{\boldsymbol{\xi}}_i} \boldsymbol{\eta}_i^r - \text{ad}_{\boldsymbol{\xi}_i} \dot{\boldsymbol{\eta}}_i^r, \quad (9)$$

where $\text{ad}_{(.)} \in \mathbb{R}^{6 \times 6}$ is the adjoint operator of $\mathfrak{se}(3)$ (see Appendix 7). By virtue of the identities $(\text{Ad}_{\mathbf{g}_i})' = \text{Ad}_{\mathbf{g}_i} \text{ad}_{\boldsymbol{\xi}_i}$, and $(\dot{\text{Ad}}_{\mathbf{g}_i}) = \text{Ad}_{\mathbf{g}_i} \dot{\text{ad}}_{\boldsymbol{\eta}_i^r}$, it can be verified that the analytic integration of (8) and (9) is given by:

$$\boldsymbol{\eta}_i^r(X_i) = \text{Ad}_{\mathbf{g}_i^{-1}} \int_0^{X_i} \text{Ad}_{\mathbf{g}_i} \dot{\boldsymbol{\xi}}_i ds, \quad (10)$$

$$\begin{aligned}\dot{\boldsymbol{\eta}}_i^r(X_i) &= \text{Ad}_{\mathbf{g}_i^{-1}} \int_0^{X_i} (\text{Ad}_{\mathbf{g}_i}) \dot{\boldsymbol{\xi}}_i ds + \\ &\quad \text{Ad}_{\mathbf{g}_i^{-1}} \int_0^{X_i} \text{Ad}_{\mathbf{g}_i} \ddot{\boldsymbol{\xi}}_i ds,\end{aligned}\quad (11)$$

(note that $\boldsymbol{\eta}_i^r(0) = \dot{\boldsymbol{\eta}}_i^r(0) = \mathbf{0}$) where $\text{Ad}_{(.)}$ is the adjoint map defined in Appendix 7. Once again, equations (8), (9), and (10), (11) hold for both, rigid and soft links. It is worth noting that in the one-dimensional joint, rigid body case, we have $\text{Ad}_{\mathbf{g}_i} \boldsymbol{\xi}_i = \boldsymbol{\xi}_i$. Thus, equations (10), (11) reduce to²¹

$$\boldsymbol{\eta}_i^r(1) = \dot{\boldsymbol{\xi}}_i, \quad \dot{\boldsymbol{\eta}}_i^r(1) = \ddot{\boldsymbol{\xi}}_i. \quad (12)$$

In all the other cases, including multidimensional joints, equations (10), (11) should be used. The absolute velocity twist of a link i in body-frame is recursively defined by:

$$\boldsymbol{\eta}_i(X_i) = \text{Ad}_{\mathbf{g}_{hi} \mathbf{g}_i}^{-1} \boldsymbol{\eta}_h + \boldsymbol{\eta}_i^r, \quad (13)$$

while its time derivative gives:

$$\dot{\boldsymbol{\eta}}_i(X_i) = \text{Ad}_{\mathbf{g}_{hi} \mathbf{g}_i}^{-1} (\dot{\boldsymbol{\eta}}_h + \text{ad}_{\boldsymbol{\eta}_h} \text{Ad}_{\mathbf{g}_{hi} \mathbf{g}_i} \boldsymbol{\eta}_i^r) + \dot{\boldsymbol{\eta}}_i^r, \quad (14)$$

where $\boldsymbol{\eta}_h$ is the velocity twist of the previous link h .

It is time now to discretize the system and introduce the generalized coordinates. The continuous strain fields $\boldsymbol{\xi}_i(X_i)$ are parametrized by a finite functional bases of strain modes¹².

$$\boldsymbol{\xi}_i(X_i) = \mathbf{B}_{\xi_i} \mathbf{q}_i + \boldsymbol{\xi}_i^*, \quad (15)$$

where $\mathbf{B}_{\xi_i}(X_i) \in \mathbb{R}^{6 \times n_i}$ (n_i being the number of degrees of freedom (DoF) of link i) is a matrix function whose columns form the basis for the strain field, $\mathbf{q}_i \in \mathbb{R}^{n_i}$ is the vector of coordinates in that basis, and $\boldsymbol{\xi}_i^*(X_i) \in \mathbb{R}^6$ is a reference strain whose primary function is to model non-zero yet constrained strains such as inextensibility. Note that the matrix $\mathbf{B}_{\xi_i}(X_i)$ is constant for rigid joints.

Fitting (15) into (10), (11) which in turn appears in (13), (14), allows finding the desired relation between the time derivatives of the generalized coordinates and the links velocity and acceleration twists.

$$\begin{aligned} \boldsymbol{\eta}_j(X_j) &= \sum_{i=0}^j \text{Ad}_{\mathbf{g}_i \cdots \mathbf{g}_j}^{-1} \int_0^{L_i \text{or} X_j} \text{Ad}_{\mathbf{g}_i} \mathbf{B}_{\xi_i} ds \dot{\mathbf{q}}_i \\ &= \sum_{i=0}^j {}^j \mathbf{S}_i \dot{\mathbf{q}}_i = \mathbf{J}_j \dot{\mathbf{q}}, \end{aligned} \quad (16)$$

$$\begin{aligned} \dot{\boldsymbol{\eta}}_j(X_j) &= \sum_{i=0}^j {}^j \mathbf{S}_i \ddot{\mathbf{q}}_i + \text{ad}_{\text{Ad}_{\mathbf{g}_i \cdots \mathbf{g}_j}^{-1} \boldsymbol{\eta}_h} {}^j \mathbf{S}_i \dot{\mathbf{q}}_i + \\ &\quad \text{Ad}_{\mathbf{g}_i \cdots \mathbf{g}_j}^{-1} \int_0^{L_i \text{or} X_j} (\text{Ad}_{\mathbf{g}_i}) \dot{\mathbf{B}}_{\xi_i} ds \dot{\mathbf{q}}_i \\ &= \sum_{i=0}^j {}^j \mathbf{S}_i \ddot{\mathbf{q}}_i + {}^j \dot{\mathbf{S}}_i \dot{\mathbf{q}}_i = \mathbf{J}_j \ddot{\mathbf{q}} + \dot{\mathbf{J}}_j \dot{\mathbf{q}}. \end{aligned} \quad (17)$$

Equations (16), (17) defines the geometric Jacobian $\mathbf{J}_j(\mathbf{q}, X_i) \in \mathbb{R}^{6 \times n}$ (n being the total number of DOFs), its time derivative $\dot{\mathbf{J}}_j(\mathbf{q}, \dot{\mathbf{q}}, X_i) \in \mathbb{R}^{6 \times n}$, and the vector of generalized coordinates $\mathbf{q} \in \mathbb{R}^n$. It is worth noting that, thanks to (12), in the one-dimensional joint, rigid body case, equations (16), (17) reduce to²¹

$$\boldsymbol{\eta}_j(1) = \sum_{i=0}^j \text{Ad}_{\mathbf{g}_i \cdots \mathbf{g}_j}^{-1} \mathbf{B}_{\xi_i} \dot{\mathbf{q}}_i = \sum_{i=0}^j {}^j \mathbf{S}_i \dot{\mathbf{q}}_i, \quad (18)$$

$$\dot{\boldsymbol{\eta}}_j(1) = \sum_{i=0}^j {}^j \mathbf{S}_i \ddot{\mathbf{q}}_i + \text{ad}_{\text{Ad}_{\mathbf{g}_i \cdots \mathbf{g}_j}^{-1} \boldsymbol{\eta}_h} {}^j \mathbf{S}_i \dot{\mathbf{q}}_i. \quad (19)$$

2.2. Dynamics

Once a Jacobian is found, the generalized dynamics of the floating hybrid chain can be obtained by projecting the free dynamics of each link by virtue of D'Alembert's principle. The free-body dynamic equations for a rigid link in the body-frame is¹⁶

$$\mathcal{M}_i \dot{\boldsymbol{\eta}}_i + \text{ad}_{\boldsymbol{\eta}_i}^* \mathcal{M}_i \boldsymbol{\eta}_i = \mathcal{F}_{J_i} - \text{Ad}_{\mathbf{g}_{ij} \mathbf{g}_j}^* \mathcal{F}_{J_j} + \mathcal{F}_{e_i} \quad (20)$$

where $\mathcal{M}_i \in \mathbb{R}^{6 \times 6}$ represents the skrew inertia matrix ($\mathcal{M}_i = \text{diag}(I_{x_i}, I_{y_i}, I_{z_i}, m_i, m_i, m_i)$ if the body frame is a principal axis frame, m_i being the body mass and $I_{\cdot i}$ the second moment of inertia), $\mathcal{F}_{J(\cdot)} \in \mathbb{R}^6$ is the wrench transmitted across joint (\cdot) , $\mathcal{F}_{e_i} \in \mathbb{R}^6$ is the concentrated external load, while $\text{ad}_{(\cdot)}^*$, $\text{Ad}_{(\cdot)}^* \in \mathbb{R}^{6 \times 6}$ are the coadjoint operator and coadjoint map respectively (see Appendix 7).

For a soft link, the free-body dynamic equation in the local frame and its boundary conditions are²⁰:

$$\begin{aligned} \bar{\mathcal{M}}_i \dot{\boldsymbol{\eta}}_i + \text{ad}_{\boldsymbol{\eta}_i}^* \bar{\mathcal{M}}_i \boldsymbol{\eta}_i &= \\ &(\mathcal{F}_{i_i} - \mathcal{F}_{a_i})' + \text{ad}_{\boldsymbol{\xi}_i}^* (\mathcal{F}_{i_i} - \mathcal{F}_{a_i}) + \bar{\mathcal{F}}_{e_i}, \\ &(\mathcal{F}_{i_i} - \mathcal{F}_{a_i})(0) = -\mathcal{F}_{J_i}, \\ &(\mathcal{F}_{i_i} - \mathcal{F}_{a_i})(L_i) = -\text{Ad}_{\mathbf{g}_{ij}}^* \mathcal{F}_{J_j}. \end{aligned} \quad (21)$$

where $\bar{\mathcal{M}}_i(X_i) \in \mathbb{R}^{6 \times 6}$ is the screw inertia density matrix of the cross-section ($\bar{\mathcal{M}}_i = \rho_i \text{diag}(J_{x_i}, J_{y_i}, J_{z_i}, A_i, A_i, A_i)$ if the local frame is a principal axis frame, ρ_i being the mass density, $A_i(X_i)$ the cross-section area, and $J_{\cdot i}$ the second moment of area), $\bar{\mathcal{F}}_{e_i}(X_i) \in \mathbb{R}^6$ is the distributed external load, and $\mathcal{F}_{i_i}(X_i), \mathcal{F}_{a_i}(X_i) \in \mathbb{R}^6$ are the internal wrenches due to the material elasticity and distributed actuation respectively. See Figure 2 for a graphical representation.

[Figure 2 about here.]

For what concerns the internal elastic wrench, one can take the derivative of any elastic energy potential that better describes the rod elasticity. Without loss of generality, a Hook-like linear elastic law is used here, which reads:

$$\begin{aligned} \mathcal{F}_{i_i}(X_i) &= \Sigma_i (\boldsymbol{\xi}_i - \boldsymbol{\xi}_i^*) + \Upsilon_i \dot{\boldsymbol{\xi}}_i \\ &= \Sigma_i \mathbf{B}_{\xi_i} \mathbf{q}_i + \Upsilon_i \mathbf{B}_{\xi_i} \dot{\mathbf{q}}_i, \end{aligned} \quad (22)$$

where $\Sigma_i(X_i) = \text{diag}(G_i J_{x_i}, E_i J_{y_i}, E_i J_{z_i}, E_i A_i, G_i A_i, G_i A_i) \in \mathbb{R}^{6 \times 6}$ is the screw elasticity matrix, E_i being the Young modulus and G_i the shear modulus (note that we have assumed the x -axis to be perpendicular to the cross-section), and $\Upsilon_i(X_i) = \text{diag}(J_{x_i}, 3J_{y_i}, 3J_{z_i}, 3A_i, A_i, A_i)\nu \in \mathbb{R}^{6 \times 6}$ is the screw damping matrix, ν being the material damping. With regards to the actuation, here we consider threadlike actuators such as tendons and embedded pneumatic chambers²². The actuation wrench is obtained by computing the force and moment exerted on the mid-line of the rod. This is given by¹²:

$$\mathcal{F}_{a_i}(X_i) = \sum_{k=1}^{n_{a_i}} \begin{bmatrix} \tilde{d}_{i_k} t_{i_k} \\ t_{i_k} \end{bmatrix} u_{i_k} = \mathbf{B}_{\tau_i} \mathbf{u}_i, \quad (23)$$

where $\mathbf{B}_{\tau_i}(\mathbf{q}_i, X_i) \in \mathbb{R}^{6 \times n_{a_i}}$ (n_{a_i} being the number of actuators of link i) is an actuation matrix, $\mathbf{d}_{i_k}(X_i) \in \mathbb{R}^3$ represents the distance from the mid-line to actuator k , $\mathbf{t}_{i_k}(\mathbf{q}_i, X_i) \in \mathbb{R}^3$ is the unit vector tangent to the actuator path, and $\mathbf{u}_i \in \mathbb{R}^{n_{a_i}}$ is the vector of magnitude actuation forces (see Figure 2).

It is now possible to obtain the generalized dynamic equation of the system via D'Alembert's principle. Projecting the continuous models (20), (21) onto the space of generalized coordinates through the Jacobians \mathbf{J}_i and integrating over the length of the soft links yields

$$\mathbf{M}\ddot{\mathbf{q}} + \mathbf{C}\dot{\mathbf{q}} + \mathbf{K}\mathbf{q} + \mathbf{D}\dot{\mathbf{q}} = \mathbf{B}\mathbf{u} + \mathbf{F}, \quad (24)$$

where $\mathbf{M}(\mathbf{q}) \in \mathbb{R}^{n \times n}$ is the mass matrix, $\mathbf{C}(\mathbf{q}, \dot{\mathbf{q}}) \in \mathbb{R}^{n \times n}$ is the Coriolis matrix, $\mathbf{D} \in \mathbb{R}^{n \times n}$ is the damping matrix, $\mathbf{K} \in \mathbb{R}^{n \times n}$ is the stiffness matrix, $\mathbf{B}(\mathbf{q}) \in \mathbb{R}^{n \times n_a}$ (n_a being the total number of actuators) is the actuation matrix, $\mathbf{F}(\mathbf{q}, \dot{\mathbf{q}}) \in \mathbb{R}^n$ is the vector of generalized external forces and $\mathbf{u} \in \mathbb{R}^{n_a}$ is the vector of applied actuation forces. These components are detailed below. For more information on the mathematical procedure, we refer the reader to Renda et al.,²³ Renda and Seneviratne¹⁷ and Renda et al.¹² Also, an extension to closed-chain systems has been re-

cently proposed in Armanini et al.,²⁴

$$\mathbf{M}(\mathbf{q}) = \sum_{i=1}^N \int_0^{L_i} \mathbf{J}_i^T \bar{\mathbf{M}} \mathbf{J}_i dX_i \quad (25)$$

$$\mathbf{C}(\mathbf{q}, \dot{\mathbf{q}}) = \sum_{i=1}^N \int_0^{L_i} \mathbf{J}_i^T \left(\text{ad}_{\eta_i}^* \bar{\mathbf{M}} \mathbf{J}_i + \bar{\mathbf{M}} \dot{\mathbf{J}}_i \right) dX_i \quad (26)$$

$$\mathbf{D} = \text{diag}_{i=0}^N \left(\int_0^{L_i} \mathbf{B}_{\xi_i}^T \Upsilon_i \mathbf{B}_{\xi_i} dX_i \right) \quad (27)$$

$$\mathbf{K} = \text{diag}_{i=0}^N \left(\int_0^{L_i} \mathbf{B}_{\xi_i}^T \Sigma_i \mathbf{B}_{\xi_i} dX_i \right) \quad (28)$$

$$\mathbf{B}(\mathbf{q}) = \text{diag}_{i=0}^N \left(\mathbf{i} \mathbf{S}_i^T \text{ or } \int_0^{L_i} \mathbf{B}_{\xi_i}^T \mathbf{B}_{\tau_i} dX_i \right) \quad (29)$$

$$\mathbf{F}(\mathbf{q}, \dot{\mathbf{q}}) = \sum_{i=1}^N \int_0^{L_i} \mathbf{J}_i^T \bar{\mathbf{F}}_{e_i} dX_i \quad (30)$$

(where N is the total number of links). With the exception of (29), the components of (24) specified above are given from a soft link point of view. However, it is easy to recover the rigid body case by removing the integrals and replacing the distributed quantities with their lumped counterparts. Also, note that in the rigid link case $\mathbf{u}_i = \mathcal{F}_{J_i}$ in general.

2.3. Constant-strain Case

To prepare the ground for the GVS computational algorithm of section 3, we propose here an improved version of the constant-strain kinematics developed in Renda et al.,²⁵ and Renda et al.²³

Assuming constant strains, the Magnus expansion in (6) takes a simple analytical form.

$$\begin{aligned} \Omega_i(X_i) &= X_i \xi_i = X_i (\mathbf{B}_{\xi_i} \mathbf{q}_i + \xi_i^*) \\ &= \mathbf{B}_{\Omega_i} \mathbf{q}_i + X_i \xi_i^*, \end{aligned} \quad (31)$$

where $\mathbf{B}_{\Omega_i}(X_i)$ has been defined. This result has a profound impact on the kinematics of a soft link. First, equation (31) can be directly applied to the PoE formula (7). For what concerns the velocity twist, we obtain the following sequence of identi-

ties starting from (10).

$$\begin{aligned}
\boldsymbol{\eta}_i^r(X_i) &= \text{Ad}_{\mathbf{g}_i^{-1}} \int_0^{X_i} \text{Ad}_{\mathbf{g}_i} ds \mathbf{B}_{\boldsymbol{\xi}_i} \dot{\mathbf{q}}_i \\
&= \text{Ad}_{\mathbf{g}_i^{-1}} \int_0^{X_i} \exp(s \text{ad}_{\boldsymbol{\xi}_i}) ds \mathbf{B}_{\boldsymbol{\xi}_i} \dot{\mathbf{q}}_i \quad (32) \\
&= \text{Ad}_{\mathbf{g}_i^{-1}} \text{T}_{\boldsymbol{\xi}_i}(X_i) \mathbf{B}_{\boldsymbol{\xi}_i} \dot{\mathbf{q}}_i \\
&= \text{Ad}_{\mathbf{g}_i^{-1}} \text{T}_{\boldsymbol{\Omega}_i}(1) \mathbf{B}_{\boldsymbol{\Omega}_i} \dot{\mathbf{q}}_i ,
\end{aligned}$$

where $\text{T}_{\boldsymbol{\Omega}}(X_i)$ is the tangent operator of the exponential map¹⁹ provided in Appendix 7. For what concerns the acceleration twist, from (11) we obtain

$$\begin{aligned}
\dot{\boldsymbol{\eta}}_i^r(X_i) &= \text{Ad}_{\mathbf{g}_i^{-1}} \int_0^{X_i} (\text{Ad}_{\mathbf{g}_i}) ds \mathbf{B}_{\boldsymbol{\xi}_i} \dot{\mathbf{q}}_i + \\
&\quad \text{Ad}_{\mathbf{g}_i^{-1}} \int_0^{X_i} \text{Ad}_{\mathbf{g}_i} ds \mathbf{B}_{\boldsymbol{\xi}_i} \ddot{\mathbf{q}}_i \\
&= \text{Ad}_{\mathbf{g}_i^{-1}} \dot{\text{T}}_{\boldsymbol{\xi}_i}(X_i) \mathbf{B}_{\boldsymbol{\xi}_i} \dot{\mathbf{q}}_i + \quad (33) \\
&\quad \text{Ad}_{\mathbf{g}_i^{-1}} \text{T}_{\boldsymbol{\xi}_i}(X_i) \mathbf{B}_{\boldsymbol{\xi}_i} \ddot{\mathbf{q}}_i \\
&= \text{Ad}_{\mathbf{g}_i^{-1}} \dot{\text{T}}_{\boldsymbol{\Omega}_i}(1) \mathbf{B}_{\boldsymbol{\Omega}_i} \dot{\mathbf{q}}_i + \\
&\quad \text{Ad}_{\mathbf{g}_i^{-1}} \text{T}_{\boldsymbol{\Omega}_i}(1) \mathbf{B}_{\boldsymbol{\Omega}_i} \ddot{\mathbf{q}}_i ,
\end{aligned}$$

where $\dot{\text{T}}_{\boldsymbol{\Omega}}(X_i)$ is the time derivative of the tangent operator of the exponential map provided in Appendix 7.

Thanks to (32) and (33), the Jacobian and its time derivative, defined in (16) and (17), can be computed analytically. The same is true for the dynamic model (24). Owing to the analogy we established between rigid joints and soft links, the constant-strain assumption holds exactly in the case of rigid joints,¹⁷ including multidimensional ones.

3. Computational Implementation

Despite its clarity, the GVS explicit approach outlined in section 2 presents several computational challenges. In the general variable-strain case, the Magnus expansion in (6) does not have a compact, finite representation. Consequently, the velocity twist (10) and acceleration twist (11) do not have an analytic expression. The same is true for the Jacobian in (16), its time derivative in (17), and, ultimately, the dynamic equation (24). In the worst case of the Coriolis matrix (26), there are four nested integrals to be evaluated numerically

starting from the strains — the configuration (1), the Jacobian (16), its time derivative (17), and the Coriolis matrix itself (26). In the following, we propose a method to approximate these integrals accurately and efficiently.

First of all, let us separate the Lagrangian matrices (25)-(30) into two groups. The mass matrix \mathbf{M} , Coriolis matrix \mathbf{C} , and generalized external forces vector \mathbf{F} are associated with absolute or "external" quantities (configuration \mathbf{g}_{si} and velocity $\boldsymbol{\eta}_i$), while the stiffness matrix \mathbf{K} and the actuation matrix \mathbf{B} are associated with relative or "internal" quantities (the strains $\boldsymbol{\xi}_i$). These two groups should be approached differently. The second group members can be computed analytically also in the general variable strain case as long the chosen bases in $\mathbf{B}_{\boldsymbol{\xi}_i}$ allow for it. In particular, the stiffness matrix associated with a linear, Hook-like, constitutive law is independent of the strain and thus can be computed offline. Note that a nonlinear, strain-dependent constitutive law can also be used within the present framework.

We now move our attention to the members of the first group. We seek to employ a Gaussian quadrature scheme to calculate the integral terms related to a soft link i . To do so, in addition to the problem data such as the screw inertia density matrix $\bar{\mathbf{M}}_i$ and the distributed external load $\bar{\mathcal{F}}_{e_i}$, the value of the configuration \mathbf{g}_{si} , Jacobian matrix \mathbf{J}_i and its derivative $\dot{\mathbf{J}}_i$ needs to be calculated at the quadrature points.

In the k^{th} interval of material length h_k between two consecutive points, the Magnus expansion can be approximated at any order following the Zanna collocation approach,²⁶ yielding the recursive formula

$$\mathbf{g}_{si}(X_i + h_k) = \mathbf{g}_{si}(X_i) \exp\left(\widehat{\boldsymbol{\Omega}}_i^k(h_k)\right). \quad (34)$$

For example, a fourth-order approximation is given by

$$\boldsymbol{\Omega}_i^k(h_k) = \frac{h_k}{2} (\boldsymbol{\xi}_{i1}^k + \boldsymbol{\xi}_{i2}^k) + \frac{\sqrt{3}h_k^2}{12} \text{ad}_{\boldsymbol{\xi}_{i1}^k} \boldsymbol{\xi}_{i2}^k, \quad (35)$$

where

$$\begin{aligned}
\xi_{i_1}^k &= \xi_i \left(X_i + h_k/2 - \sqrt{3}h_k/6 \right) \\
&= \mathbf{B}_{\xi_i} \left(X_i + h_k/2 - \sqrt{3}h_k/6 \right) \mathbf{q}_i \\
&= \mathbf{B}_{\xi_{i_1}}^k \mathbf{q}_i \\
\xi_{i_2}^k &= \xi_i \left(X_i + h_k/2 + \sqrt{3}h_k/6 \right) \\
&= \mathbf{B}_{\xi_i} \left(X_i + h_k/2 + \sqrt{3}h_k/6 \right) \mathbf{q}_i \\
&= \mathbf{B}_{\xi_{i_2}}^k \mathbf{q}_i
\end{aligned} \tag{36}$$

are the quadrature points of the Zanna collocation method. Thus, a two-level nested quadrature scheme is used, which resembles the orthogonal collocation method of Orekhov and Simaan.²⁷

Now, equation (34) jumps from one point to the next as a constant-strain section of length h_k and strain $\Omega_i^k(h_k)/h_k$ would do. Motivated by this analogy, we seek to apply equations (32) and (33) to the interval k . Let us take the time derivative of $\Omega_i^k(h_k)$. For example, at the fourth-order approximation, we obtain

$$\begin{aligned}
\dot{\Omega}_i^k(h_k) &= \frac{h_k}{2} \left(\dot{\xi}_{i_1}^k + \dot{\xi}_{i_2}^k \right) + \\
&\quad \frac{\sqrt{3}h_k^2}{12} \left(\text{ad}_{\dot{\xi}_{i_1}^k} \xi_{i_2}^k + \text{ad}_{\dot{\xi}_{i_1}^k} \dot{\xi}_{i_2}^k \right) \\
&= \frac{h_k}{2} \left(\mathbf{B}_{\xi_{i_1}}^k + \mathbf{B}_{\xi_{i_2}}^k \right) \dot{\mathbf{q}}_i + \\
&\quad \frac{\sqrt{3}h_k^2}{12} \left(\text{ad}_{\dot{\xi}_{i_1}^k} \mathbf{B}_{\xi_{i_2}}^k - \text{ad}_{\dot{\xi}_{i_2}^k} \mathbf{B}_{\xi_{i_1}}^k \right) \dot{\mathbf{q}}_i \\
&= \mathbf{B}_{\Omega_i}^k \dot{\mathbf{q}}_i,
\end{aligned} \tag{37}$$

which defines $\mathbf{B}_{\Omega_i}^k(h_k)$. Then, (32) and (33) become

$$\boldsymbol{\eta}_i^r(h_k) = \text{Ad}_{\exp \widehat{\Omega}_i^k}^{-1} \mathbf{T}_{\Omega_i^k} \mathbf{B}_{\Omega_i}^k \dot{\mathbf{q}}_i, \tag{38}$$

$$\begin{aligned}
\dot{\boldsymbol{\eta}}_i^r(h_k) &= \text{Ad}_{\exp \widehat{\Omega}_i^k}^{-1} \dot{\mathbf{T}}_{\Omega_i^k} \mathbf{B}_{\Omega_i}^k \dot{\mathbf{q}}_i + \\
&\quad \text{Ad}_{\exp \widehat{\Omega}_i^k}^{-1} \mathbf{T}_{\Omega_i^k} \mathbf{B}_{\Omega_i}^k \ddot{\mathbf{q}}_i,
\end{aligned} \tag{39}$$

where the velocity and acceleration twists are measured relative to the quadrature point at the beginning of interval k .

Fitting (38), (39) into (16), (17) produces a recursive formula for the Jacobian and its time

derivative for the general GVS approach.

$$\begin{aligned}
\mathbf{J}_i(X_i + h_k) &= \text{Ad}_{\exp \widehat{\Omega}_i^k}^{-1} \left(\mathbf{J}_i(X_i) + \right. \\
&\quad \left. \left[\mathbf{0}_{6 \times n_i^-} \mathbf{T}_{\Omega_i^k} \mathbf{B}_{\Omega_i}^k \mathbf{0}_{6 \times n_i^+} \right] \right), \tag{40}
\end{aligned}$$

$$\begin{aligned}
\dot{\mathbf{J}}_i(X_i + h_k) &= \text{Ad}_{\exp \widehat{\Omega}_i^k}^{-1} \left(\dot{\mathbf{J}}_i(X_i) + \right. \\
&\quad \left. \left[\mathbf{0}_{6 \times n_i^-} \left(\text{ad}_{\boldsymbol{\eta}_i(X_i)} \mathbf{T}_{\Omega_i^k} + \dot{\mathbf{T}}_{\Omega_i^k} \right) \mathbf{B}_{\Omega_i}^k \mathbf{0}_{6 \times n_i^+} \right] \right), \tag{41}
\end{aligned}$$

where $n_i^- = \sum_{l=0}^{i-1} n_l$ and $n_i^+ = \sum_{l=i+1}^N n_l$. To pass from one link to the next one can use

$$\mathbf{J}_j(0) = \text{Ad}_{\mathbf{g}_{ij}^{-1}} \mathbf{J}_i(L_i), \tag{42}$$

$$\dot{\mathbf{J}}_j(0) = \text{Ad}_{\mathbf{g}_{ij}^{-1}} \dot{\mathbf{J}}_i(L_i) \tag{43}$$

In conclusion, a two-level nested quadrature scheme has been presented to compute all the Lagrangian matrices (25)-(30). Figure 3 provides a graphical representation of the numerical scheme for a single soft link.

[Figure 3 about here.]

Although it can be applied to the constant-strain case too, the above method should not be confused with a piece-wise constant-strain approach. First, there is a single set of coordinates for an entire soft link instead of a different set for each interval between two quadrature points. Second, the Zanna approximation provides higher-order jumps between two consecutive points.

4. Overview of the SoRoSim Toolbox

The programming approach used in creating this toolbox is Object-Oriented Programming (OOP). This approach entails software design around data, or objects, rather than functions and logic. In OOP, the developer groups “Objects” having similar attributes or that require similar manipulations together under a class. The user can then insert data in the form of ‘Properties’ associated with that specific object. After an object is created, various functions or ‘Methods’ can be defined within the class to perform manipulations on the object to yield required results. This type of programming is well-suited for programs that are large, complex and actively updated or maintained.²⁸

OOP comes with many advantages as it provides a well-structured map of the program and allows easy access and adjustment to object-specific data. OOP also allows re-usability, once an object is defined and saved in MATLAB's work space the user can perform multiple manipulations without having to re-define the object.

The SoRoSim toolbox consists of three classes, namely Link, Twist, and Linkage, that work together to form a powerful simulation tool that employs the geometrical variable strain model to analyze soft, rigid, and hybrid open-chain manipulators. The toolbox was validated by comparing results with verified static models from Renda et al.,¹² and dynamic models such as those in Boyer et al.¹³ Experiments were also set up and used to validate the dynamic and static analysis results of the toolbox. In this section, we discuss the properties and methods of each class and demonstrate an example for using the toolbox.

4.1. The Link Class

A link is considered as a rigid or a soft body which is attached to a lumped joint at its starting position. The Link class allows the user to construct links that could later be combined to form manipulators. The Link class makes use of 'Properties' to define link parameters. Some properties are user-defined, some are default values, while others are automatically computed. An element of the Link class is an OOP object derived from handle. It is always passed as reference, i.e., MATLAB allows a function to make changes to the variable in-place without the need for a copy. We divide the properties associated with this class into three categories: General Properties, Geometric Properties, and Material Properties (Table. 1).

[Table 1 about here.]

Properties that defines the general characteristic of the link are grouped together as General Properties. These properties include the type of lumped joint (`jointtype`), body type (`linktype`), cross sectional shape (`CS`), number of pieces on the link (`npie`), and Gauss quadrature parameters (`nGauss`, `Xs`, and `Ws`). For a rigid link, `npie` is 1, which corresponds to the joint, while for a soft link, `npie` is

equal to the total number of divisions plus 1. `nGauss{division_number}` indicates the total number of points on a soft division at which the toolbox performs computations (significant points). It includes the start and endpoints of the division in addition to the Gauss quadrature points. `Xs` and `Ws` are corresponding normalized positions and weights.

Properties that are related to the geometry of the link fall under Geometric Properties. Properties such as the piece-wise length of soft link divisions (`lp`), total length of the link (`L`), radius (`r`) of a link with a circular cross section, width (`w`) and height (`h`) of a link with a rectangular cross section, and coordinates of origin with respect to the previous frame (`cx`, `cy`, and `cz`) are geometric properties of the Link class. The Link class saves the radius, height, and width as functions of `X1`, where `X1` varies from 0 to 1. For a rigid link, the Geometric Properties are saved as numerical values, while for the soft link they (with the exception of `L`) are saved as cell elements with a numerical value for each division of the link. For instance, to access the radius of a rigid link, the syntax is `L1.r` while for a soft link, it is `L1.r{division_number}`, where `L1` is the name of the Link class element.

Material Properties include the employed material's Young's modulus (`E`), Poisson's ratio (`Poi`), density (`Rho`), and material damping (`Eta`). For a rigid link, only the value of `Rho` is significant. Using these values along with the Geometrical Properties of the Link, the program computes the shear modulus (`G`), the screw inertia matrix (`Ms`), screw stiffness matrix (`Es`), and screw damping matrix (`Gs`). These derived quantities are also saved as the Material Properties of the link. For a rigid link, `Ms` represents the screw stiffness matrix of the whole body (\mathcal{M}). In contrast, for a soft link, `Ms`, `Es`, and `Gs` represent the cross-sectional inertia ($\bar{\mathcal{M}}$), stiffness (Σ), and damping matrices (Υ) computed at every significant point of each division. The Link class saves them as cell elements.

The Link class also includes Plot Properties that are used to plot the link. They include the number of cross sections (per division) of the link (`n_l`), the number of radial points (`n_r`, applicable only for a circular cross section), and the

color of the link (`color`). The user can choose a color that follows the MATLAB color code. The default values of `n_l`, `n_r` and `color` are '10', '18', and 'b' (blue) respectively.

To create a Link, the syntax is `LinkName = Link`. Then the user needs to follow the dialog boxes that appear. Default values are provided for all properties if the user do not wish to change. Figure 4 shows the step by step process for creating a soft and a rigid link. Once a Link is created, the 'dot' indexing allows to access or modify its properties. For instance, to change the color of the link `L1` to red, the syntax is `L1.color='r'`. Changing a property of the Link class will affect all its dependent properties. For example, a change of the radius of the second division of a soft link `L1` by `L1.r{2}=new_value` will update the values of `L1.Ms{2}`, `L1.Es{2}`, and `L1.Gs{2}`.

[Figure 4 about here.]

4.2. The Twist Class

We define a 'piece' as a joint or a division of the soft link within the open-chain manipulator. The Twist class is used to specify the allowable degrees of freedom (DoFs) of each piece. For lumped joints (rigid joints), the Twist class creates a base matrix (`B`, as shown in Table. 2) with '1's' and '0's', where '1' indicates that a particular DoF is allowed. `B` is a property of the twist class.

[Table 2 about here.]

For a division of a soft link (distributed system), there are six modes of deformation: torsion about x axis, bending about y axis, bending about z axis, elongation about x axis, shear about y axis and shear about z axis. We use a property of Twist class, namely `Bdof`, to specify the allowable modes. `Bdof` is a 6×1 array of '1's' and '0's', where 1 indicates that a particular deformation mode is allowed and 0 indicates that it is not. Another property called `Bodr`, which is also a 6×1 array, specifies the order of polynomials that are used to fit the strains corresponding to each deformation mode. Using `Bdof` and `Bodr`, the Twist class computes the base matrix (`B`) of a soft division at every Gauss quadrature points (`Xs`) of the

division. Some of the most commonly used Base matrix for a distributed system are shown in Table. 3.

[Table 3 about here.]

Properties namely `B_Z1` and `B_Z2` are base matrices that are evaluated at points associated with the forth-order Zanna's collocation method. The Twist class saves the reference strain vector corresponding to a piece ($\xi^*(X)$) as a property namely `xi_starfn`. Another property called, `xi_star`, saves the value of $\xi^*(X)$ at points associated with Gauss quadrature and Zanna's collocation method. Finally, the total number of joint coordinates required to specify the state of a piece is saved as a property called `dof`.

The Twist class is called during the creation of the Linkage class element. The Linkage class collects the Twist class elements of each piece and saves them together as a Twist vector. Hence, the Twist class elements are accessed through the Linkage class element. Table. 4 summarizes the properties of Twist class.

[Table 4 about here.]

4.3. The Linkage Class

The Linkage class allows the user to combine previously defined Link class elements into a serial open-chain manipulator (linkage). The Linkage class allows the user to apply external or actuation loads to the linkage. There are in-built functions to apply external loads such as gravity and point force/moment. The user can also add custom external wrenches on the Linkage to simulate other types of external forces such as fluid interaction or contact forces.

The class consists of in-built functions to actuate all kinds of rigid joints as well as soft links. The user can actuate the joints by specifying the value of joint coordinates as a function of time or by entering the joint wrenches. Hence, the toolbox can simulate a mixed forward-inverse model for linkages with rigid joints. Built-in functions are available on the toolbox to allow users to add thread-like actuators on a soft link. We can use them to simulate actuation forces due to cables embedded inside the soft link, pneumatic actuation, and soft gripper actuation. In addition, the

user can apply custom actuator strengths or custom actuation wrenches on the soft links to simulate closed-loop control and other types of actuators.

We use the Linkage class to perform static and dynamic simulations. During the simulation, we perform the computations of soft pieces after normalizing the piece. The normalization process starts with transforming the length of a soft piece to 1 unit. Consequently, for the computation of the piece, we scale all quantities with length dimension using the original length of the piece. Hence, internally, the toolbox performs the computation of a soft piece using scaled quantities. Once the simulation is completed, the joint coordinates of soft pieces are scaled back to their original dimensions. The normalization of soft pieces avoids poorly scaled matrices such as the base matrix. This allows faster static solutions and stable dynamic simulations.

We divide the properties of the Linkage class into four main categories: General Properties, External Force Properties, Actuation Properties, and Elastic Properties. (Table. 5).

[Table 5 about here.]

4.3.1 General Properties

The General Properties of the Linkage class include numbers such as, the total number of links combined (N), total number of pieces within the linkage (n_{tot}), total number of joint coordinates to represent the state of the linkage ($ndof$), and the total number of significant points on the linkage at which the toolbox performs computations in a static or a dynamic simulation (n_{sig}). We consider joints, the center of mass of rigid links, and the significant points of soft links as the significant points of the linkage.

The Linkage class arranges the Link class elements and the Twist class elements as vectors (class arrays) and saves them as General Properties, namely `VLinks` and `Vtwists`. The properties of the Link and the Twist classes can be accessed through these properties. For example, to access the reference strain vector of the second piece of the linkage, the syntax is `S1.Vtwists(2).xi_starfn` while to access the color of the second link of the linkage, the

syntax is `S1.VLinks(2).color`, where `S1` is the name of the Linkage class element.

The linkage class computes the total length of the linkage (L_{tot}) by adding the lengths of each link. It also falls under the category of General Properties. The initial transformation matrix (`g_ini`) specifies the location and orientation of the starting frame of the linkage relative to the global frame. Similar to `g_ini` for the linkage, each piece has an initial transformation matrix. The Linkage class saves these transformation matrices as cell elements, called `g0`. Each element of `g0` (`g0{piece_number}`) corresponds to the initial transformation matrix of a piece relative to the previous frame. We include `g_ini` and `g0` in the General Properties of the Linkage class. Finally, the scaling factor of joint coordinates (`q_scale`), which is used to obtain the original joint coordinates after the static or the dynamic simulation, is also a General Property of the Linkage class.

4.3.2 External Force Properties

We organize all properties used to apply external forces or moments on the linkage as External Force Properties. The Linkage class use properties called `Gravity` and `G` to define distributed external forces such as gravity. We can enable or disabled the gravity by typing `S1.Gravity=1` or `S1.Gravity=0`. To update the magnitude and direction of the gravity, we can change the gravity wrench vector (`G`).

Similar to `Gravity`, the Linkage class uses a property called `PointForce` to enable or disable the application of point forces and moments. `np`, `Fp_loc`, and `Fp_vec` are Linkage class properties that determine the number of point forces, cell element of piece numbers corresponding to the application of point wrenches, and cell element with the magnitudes of point wrenches. Note that if we choose a rigid piece, the program will apply the point wrench at the center of mass provided by the `cx` of the Link. While, if we choose a soft piece, the program will apply the same at the tip of the piece. Hence, the user needs to divide the soft link appropriately to adjust the point of application of the wrench. During the creation of a Linkage, the program prompts users to enter the value of these properties.

Apart from these, the user can also apply a customized external wrench to the linkage. To do that, firstly, the user needs to enable the custom external force property called, `CEFP` by typing, `S1.CEFP=1` . The default value of `CEFP` is 0. Secondly, the user needs to modify a MATLAB function given by ‘CustomExtForce.m’ inside a folder, namely ‘Custom.’ The MATLAB function `CustomExtForce.m` lets the user apply a customized external wrench as a function of the `Linkage` class element, time, q , \dot{q} , g , J , η , and \dot{J} . Here, g , J , η , and \dot{J} are transformation matrices, Jacobians, screw velocities, and time derivatives of Jacobians evaluated at every significant point. Using the MATLAB function, the user can apply a point wrench on rigid links and a distributed wrench on soft links. The user can also modify a property called added mass (`M_added`) to simulate an external wrench that depends on $\dot{\eta}$. In section 6, we show an example of how we can use the customized external force to model the underwater propagation of a flagellate soft robot.

4.3.3 Actuation Properties

We classify all properties used to define actuators on the linkage as Actuation Properties. The `Linkage` class uses a property called `Actuated` to enable or disable actuation. Another property called, `nact` saves the number of actuators on the linkage. To define the actuation of lumped joints, the class uses properties such as `Bqj1`, `n_jact`, `n_jact`, `i_jactq`, and `WrenchControlled`. `Bqj1` is the generalized actuation matrix of all joints with a single degree of freedom. The property, `n_jact` saves the total number of joint actuators. `i_jact` saves the indices of Links whose joints are actuated and `i_jactq` saves the indices of joint coordinates corresponding to the lumped joints that are actuated. The property called, `WrenchControlled` is a $(n_{jact} \times 1)$ array that determines whether a wrench or joint coordinates controls the rigid joint. Using this property the toolbox can simulate mixed forward-inverse model for linkages with rigid joints.

The `Linkage` saves the number of soft actuators using a property called `n_sact`. To compute the generalized actuation matrix for the soft piece the `Linkage` class uses properties such as,

`dc`, `dcp`, `Sdiv`, `Ediv`, and `Inside`. `dc` is a $(n_{sact} \times N)$ is cell-matrix whose elements are cell arrays for a particular actuator and a link. They include the local positions of the actuator path in the format $[0, y_p, z_p]^T$ at every significant point of each soft division. `dcp` saves the derivative of local cable positions in a similar way. The user can choose the actuator path from the list: ‘constant’, ‘oblique’, ‘helical’, and ‘custom’. `Sdiv` and `Ediv` are also cell matrices with the data of division numbers corresponding to the start and the end position of an actuator on a link. The property called, `Inside` determines whether the actuator is fully embedded inside the linkage or is partially outside. The value of this property is 1 if the actuator is fully inside and 0 if it is not. The toolbox uses the later case to simulate the actuation of soft grippers. We show an example of the simulation of a soft gripper in section 6. The toolbox estimates the value of all these parameters based on user inputs during the `Linkage` creation.

The toolbox prompts for the value of the actuator strength before the static or dynamic simulation. However, the user may apply a customized actuator strength on joint and soft actuators. To do this, the user needs to enable the custom actuator strength by changing the value of property called `CAS` to 1. `CAS` has a default value of 0. Subsequently, the user needs to modify a MATLAB function given by ‘CustomActuatorStrength.m’ inside the folder, namely ‘Custom.’ In the file, the user has access to the `Linkage` class element, time, q , \dot{q} , g , J , η , and \dot{J} . This opens up the possibility of simulating a closed-loop control for the linkage.

In addition to this, the user can also add a customized actuation on soft links. An Actuation Property called `CAP` is used to enable (value 1) or disable (value 0) customized actuation. `CAP` has a default value of 0. The process is similar to adding the customized external wrench. The user needs to modify a MATLAB function given by ‘CustomActuation.m’ inside the folder, namely ‘Custom.’ Similar to the ‘CustomExtForce.m’ and ‘CustomActuatorStrength.m’, in the file ‘CustomActuation.m’, the user has access to the `Linkage` class element, time, q , \dot{q} , g , J , η , and \dot{J} . Using the MATLAB function and these inputs, the user can simulate other kinds of soft actuators.

4.3.4 Elastic and Other Properties

Constant parameters such as generalized stiffness matrix and generalized damping matrix are pre-computed and saved as properties of the Linkage, namely, K and D . The class uses a property called `Damped` to enable (value 1) or disable (value 0) the elastic damping of soft links. The default value of `Damped` is 1.

We reserve three customizable properties, `CP1`, `CP2`, and `CP3`, which can be used to save constant properties of the linkage for applying a custom external force or actuation. The Linkage class also has two other properties, namely `CablePoints` and `PlotParameters`. The class uses `CablePoints` for plotting the actuator path, and `PlotParameters` is a struct element of MATLAB with parameters for changing the output plot of the simulation. The user can access the plot parameters by typing `S1.PlotParameters` and can change the value of its fields according to the formats displayed.

4.3.5 Methods of Linkage Class

Methods of a class use the properties of the class element to generate meaningful results. The Linkage class uses methods `statics` and `dynamics` to perform static and dynamic simulations. Once we create a Linkage (`S1`), the syntax for using these methods are `S1.statics` and `S1.dynamics`.

Apart from these, we pack the Linkage class with several other methods. For instance, we can use a method called `FwdKinematics` to obtain the transformation matrices at every significant point of the linkage for a given value q . The syntax is `S1.FwdKinematics(q)`, where q is a joint coordinate vector. The output is `n_sig` transformation matrices that are arranged as column arrays. Similary, to obtain the generalized coriolis matrix the syntax is `S1.GeneralizedCoriolisMatrix(q, qd)`, where q and qd are q and \dot{q} . `S1.plotq(q)` generates the shape of the open-chain manipulator for a given value of q . We provide the complete list of methods of the Linkage class in Table. 6.

[Table 6 about here.]

The syntax for creating a Linkage is

`LinkageName = Linkage(L1, L2, ...)` , where L_1 , L_2 , etc. are the names of links that are connected in series from the base to the tip. The current version of the SoRoSim toolbox (version 2.32 at the time of writing this paper) is available at mathworks.com²⁹ for free download. In the next section, using an example, we detail the process of creating a Linkage.

4.4. Linkage Creation

Let L_1 and L_2 be the soft and the rigid Links created in section 4.1 (Figure. 4). Let us change the color of L_2 by `L2.color='r'` . To create a linkage using these two links the syntax is `S1 = Linkage(L1, L2)` , where $S1$ is the name of the Linkage. This is followed by a set of dialog boxes and graphical user interfaces (GUIs) to obtain the properties of the Linkage class. The toolbox computes all General Properties of the Linkage except `Vtwists`, `ndof`, and `q_scale` using the Link class elements L_1 and L_2 . User input is required to define these properties.

4.4.1 Twist Class Definition

The first set of GUIs obtains the Twist class element for each piece on the linkage (Figure. 5). We enable all three rotational modes of deformation for the soft pieces (steps 1 and 2). For the first piece, we use a linear strain (order 1), and for the second, we keep constant strain (order 0). We also change the reference strain twist vectors for both the soft pieces, as shown in the figure (steps 1 and 2). The user may also write the reference strain vector as a function of X . For the revolute joint, we choose the y -axis as the axis of rotation (step 3).

The image of the linkage will update based on the changes we make. Once the Linkage class collects all the Twist class elements for each piece, an image of the final geometry of the link with a dialog box asking to confirm the geometry will appear (step 4). The GUI will repeat the previous steps if the user chooses ‘No’.

[Figure 5 about here.]

4.4.2 External Force Definition

Once the user confirms the geometry, the second set of GUIs appears (Figure. 6). Their purpose is to obtain the external forces or moments on the linkage. For this example, we enable Gravity in step 1 and choose ‘-y’ as the gravity direction in step 2. The toolbox assigns G with the common value of acceleration due to gravity ($9.81 m/s^2$) in the direction chosen by the user.

In steps 3 and 4 we enable PointForce and choose to apply 1 point wrench ($np = 1$). In step 5, we apply a point force of 5 N in the direction of the local y-axis at $X = 0.3$ m of the first link by choosing the piece number corresponding to the point of application of force/moment as ‘2’. Note that we can apply the point force at $X = 0.3$ m as the length of the first division of the link was 0.3 m. The Linkage class updates the value of F_{p_loc} and F_{p_vec} in this step. The user can also apply a time-varying point wrench by entering the wrench components as a function of t (time).

[Figure 6 about here.]

4.4.3 Actuation Definition

The third set of GUIs is for collects the Actuation Properties of the Linkage class (Figure. 7 and Figure .8). We enable Actuated in the first step (Figure. 7). Consequent prompts are for setting all the rigid joints on the linkage as active or passive. The GUI will highlight the links corresponding to the joint as shown in step 2. There are two ways of actuating a rigid joint, either by joint wrenches or by joint coordinates. The toolbox prompts for this in step 3. The Linkage class updates the values of B_{qj1} , n_jact , n_jact , i_jactq , and WrenchControlled in this step. For this example, we actuate the revolute joint of the rigid link by joint coordinates. The toolbox displays the image of the linkage with the letter ‘W’ on the joints that are wrench controlled and the letter ‘Q’ on the joints controlled by joint coordinates.

[Figure 7 about here.]

After every rigid joint, if there are any soft links in the linkage, the GUI asks whether the soft links are actuated (step 4 in Figure .8). After the number of soft actuators (n_sact) is up-

dated in step 5 (for this case $n_sact = 1$), the GUI prompts the user to choose whether an actuator is entirely inside the linkage or not (step 6). After this, the user needs to choose the actuator path for each actuator on each link from the list: ‘None’, ‘Constant’, ‘Oblique’, ‘Helical’, and ‘Custom’ (step 7). The option ‘None’ is to disable the actuation of the link, while the option ‘custom’ is to enter the actuator path as a function of X . For this demonstration, we choose the helical path and enter the parameters as shown in step 8. The actuator path, according to the user input, will be displayed on the linkage image (step 9). The user may change the actuator path by repeating steps 7 and 8. When step 9 is finished, the toolbox updates the rest of Actuation Properties.

[Figure 8 about here.]

In the final stage of the Linkage creation, if there are any revolute or prismatic joints within the linkage, dialog boxes asking the linear stiffness values of these joints will appear as shown in step 1 in Figure. 9. These values are used to update the generalized stiffness matrix K of the linkage. A revolute joint with a positive stiffness will act like a torsional spring, while a prismatic joint with a positive stiffness will act like a linear spring. For this example we keep the stiffness value of the revolute joint as 0 Nm/rad. Once the Linkage creation is complete, the toolbox displays its final image.

[Figure 9 about here.]

We can perform static and dynamic simulations of the linkage using the Linkage class element ($S1$) we created. We demonstrate these in the next section.

4.5. Static and Dynamic Simulation

The syntax to perform a static equilibrium simulation is $S1.statics$ . Followed by this, the toolbox prompts the user to enter the actuation parameters. For the Linkage we created, the first prompt is to enter the value of angle of the revolute joint of link 2 in radians, and the second is to enter the strength of the soft actuator 1 in Newtons. As an example, we enter ‘-pi/2’ as the revolute joint angle and ‘-200’ as the strength of the actuator. A negative value of

actuator strength implies that the actuator is acting like a cable that applies a tension. This is followed by a dialog box asking for the initial guess of the simulation. The initial guess includes the guess value of joint coordinates and the wrenches of joints which are controlled by joint coordinates.

Once the user enters the initial guess, the toolbox estimates the equilibrium state of the linkage using the nonlinear solver of MATLAB called, ‘fsolve’ and displays the output. Figure. 10 compares the equilibrium state of the linkage with its reference state. The toolbox also saves the results of the static simulation, value of joint coordinates (with a variable name ‘q’), and actuator forces (with a variable name ‘u’), in a MATLAB file called ‘StaticsSolution.mat’.

[Figure 10 about here.]

Similarly, to perform the dynamic simulation of the linkage, the syntax is `S1.dynamics` . Subsequently, the toolbox prompts the user to enter the actuation parameters for the dynamic simulation as a function of ‘t’ (time). As an example, we can input the revolute joint angle as a periodic function (`pi/2*sin(2*pi*t)`) and the actuator strength as a ramp input that goes from 0 to -200 N in one second and stays at -200 N after that (`(-200*t + (200*t-200)*heaviside(t-1))`). After this, a dialog box pops up asking for the initial condition of the simulation, which includes the initial value of joint coordinates and their time derivatives, and the simulation time. We simulate this example by keeping the default values.

The toolbox uses the differential solver of MATLAB called `ode45` to solve dynamic problems. Once the dynamic simulation is complete, another dialog box appears and asks if the user needs the output video of the simulation. If the user chooses ‘Yes’, the toolbox plots the linkage states and generates an output video in ‘.avi’ format. The toolbox saves the video as ‘Dynamics.avi’ on the folder from which we run the simulation. It also saves the dynamic simulation results in a MATLAB file called ‘DynamicssSolution.mat’. The MATLAB file will have a $(N_{dyn} \times 1)$ array of time (with a variable name ‘t’) and a $(N_{dyn} \times 2ndof)$ matrix of joint coordinates and their derivatives (with a variable name ‘qqd’,

which represents q and \dot{q}). Here, N_{dyn} is the number of elements in ‘t’ and $ndof$ is the DoF of the linkage. Figure. 11 shows the states of the linkage at different times of the dynamic simulation.

[Figure 11 about here.]

5. Numerical Tests

To validate the performance of the toolbox, we conduct several numerical and an experimental tests. We compare the results of systems modelled using the toolbox to the published and verified results while the experimental test is done by comparing the toolbox simulation results to the experimental results of a physical system.

One example of the numerical tests performed was the comparison of the bending of a clamped beam with a follower tip force to the results from test 2 of Boyer et al.³⁰ Using the toolbox, we constructed A 100m long cylindrical beam with a Young’s Modulus of $E = 6.7510^9$ Pa and a diameter of 57cm. We used a 4th order bending about the y-axis to model the deflection of the rod when subjected to a follower tip force. The rod was subjected to forces varying from 0 to 130 kN. Figure 12 shows the deflection of the link as modeled by the toolbox. The static simulation results run by the toolbox precisely match with those obtained in (Boyer et al.)³⁰

[Figure 12 about here.]

We investigated the energy balance in a damped and an undamped cantilever beam released from rest and subjected to gravity. We created a soft link with a length of 0.5 m and we vary its radius linearly from 2 cm to 1 cm. The Young’s Modulus of the link was 1×10^6 Pa and the modes of deformation allowed were: torsion and rotations about y and z-axis. We used a cubic order polynomial to simulate these modes. We run the dynamic simulation for 5 seconds. Figure. 13 shows the motion of the damped (a) and the undamped rod (b) between time, $t=0$ s to 0.75s. To obtain a complex dynamic motion, we release the soft link is released from rest with an initial bending of 1 rad/m about the y-axis.

[Figure 13 about here.]

The values of the kinetic energy, the gravitational potential energy, and the elastic potential

energy at a given time were calculated and added as shown in equation 44, where, gr is acceleration due to gravity and r_{y_i} is the y coordinate of a cross section of the rod. On the right-hand side of the equation, the first, second, and third terms represent kinetic, gravitational potential, and elastic potential energies.

$$\begin{aligned} E_{tot} = & \sum_{i=1}^N \frac{1}{2} \int_0^{L_i} \boldsymbol{\eta}_i^T \bar{\mathcal{M}} \boldsymbol{\eta}_i dX_i + \\ & \sum_{i=1}^N \int_0^{L_i} \rho_i A_i gr.r_{y_i} dX_i + \\ & \sum_{i=1}^N \frac{1}{2} \int_0^{L_i} (\boldsymbol{\xi} - \boldsymbol{\xi}^*)_i^T \boldsymbol{\Sigma}_i (\boldsymbol{\xi} - \boldsymbol{\xi}^*)_i dX_i \end{aligned} \quad (44)$$

For the undamped case, the system's total energy should remain the same as the initial elastic energy. While for the damped case, the total energy should decrease monotonically. Figure 13(c) shows a plot of the values of various forms of energies of the system. The total energy of the damped system is decaying, and that of the undamped system remains a non-zero positive constant as expected.

6. Applications

In this section, we explore and demonstrate different applications of the toolbox in various fields of research by simulating different kinds of open-chain linkages. An important study one could look at is path planning of a soft link using cable actuation. This could have many applications such as an endoscope path plan in the medical field or a collision-free navigation of soft robots through an obstacle courses. To demonstrate this we modelled, two soft, cable-actuated links. The first soft link explores the use of the toolbox to model a wide variety of cable paths. Figure 14(a) shows a cable path can be defined using the 'Custom' path option in the toolbox and Figure 14(b) shows the results of a static simulation run for the same cable when an actuator strength of -250N is applied.

[Figure 14 about here.]

The second example we explore is the use of cable actuation in path planning and guiding the tip of a given system to a desired position. Figure 15 shows how multiple cables could be used to guide the tip of a soft link to a desired location (green box) while avoiding an obstacle (red box). We used three set of cables for this particular example.

[Figure 15 about here.]

Another application that could be explored using the toolbox is the use of soft robotics in marine exploration. Due to their compliant nature soft robots pose no risk to underwater habitat or organisms which makes them a very good choice to employ in underwater exploration. In Calisti et al.,³¹ a simple underwater soft robotics propeller inspired by bacterial flagella was presented and modelled using the PCS approach. The propeller consists of a soft conical element, the *filament*, connected to a pre-curved cylindrical body, the *hook*, which is connected to a rotating motor. As the motor rotates, the soft flagella interacts with the environment assuming an helical shape that finally propels the robot. Here, the Toolbox is employed to model an analogous system, which combines 4 links: the body, representing the rigid shell containing the electronics components, the motor's shaft, the *hook* and the soft *filament*. The dimensions used to model the soft robot components were taken from Armanini et al.,³² A passive prismatic joint that allows motion along the x-axis was attached to the body of the device and an active angle controlled revolute joint was used for the shaft to model the motor. The toolbox allows the user to add custom forces through by enabling the CEF of the Linkage class. Using the 'CustomExtForce.m' file, we modelled the action of the fluid on the propeller through a drag and a lift force components, as described in.³² The motion of the shaft is angle controlled using equation $\theta = 5.1t$, where the angular velocity is 5.1 rad/s.

A dynamic simulation was run for 10 seconds, figure 16 shows super imposed images of the motion of the robot.

[Figure 16 about here.]

Users can also make use of the ability to model both soft and rigid links as well as the wide variety of lumped joints supported by the toolbox to

explore different open-chain designs. An arbitrary example of one such open-chain is shown in figure 17. The linkage shown in the figure consists of two links, a rigid link with an actuated revolute joint and a soft link with a passive spherical joint. The soft link has 4 modes of motion

[Figure 17 about here.]

Finally, we show a real example of the hybrid case by modeling a re-configurable soft gripper, namely the ReSoft gripper (Figure. 18a).³³ The gripper fingers are cable-driven and the re-configuration of the fingers is realized through revolute joints. We simulate the gripper as a combination of three linkages. The middle finger is simply a stationary soft link, while the other two consist of soft links attached to rigid links with revolute joints. The revolute joints of the rotating fingers of the ReSoft gripper are coupled in a way that if they rotate symmetrically about the stationary finger. Similarly, the gripper applies the cable tension in a way that all three fingers deform equally. We adopted a simplified design of the actual dimensions listed in Anup et al.,³³ and allowed the bending about the z-axis as the mode of deformation.

We simulate the static equilibrium of the gripper by entering the appropriate values of revolute joint angle and the cable tensions for each finger. Figure. 18b shows the simulation result of the gripper for different finger orientations.

[Figure 18 about here.]

7. Conclusion

This paper presented SoRoSim, a MATLAB toolbox that uses the Geometric Variable Strain (GVS) approach to provide a unified framework for modeling, analysis, and simulation of soft, rigid, and hybrid soft-rigid open-chain manipulators. The paper discussed the theory and the computational implementation behind the toolbox in detail. The paper can be used as a user manual of the toolbox as it covers the overview of the toolbox and provides instructions on using the toolbox features. We validated the toolbox simulation results via numerical tests and provided a substantial number of toolbox applications.

The SoRoSim version 2.32 is an initial version of the toolbox. We will be constantly improving the toolbox by enhancing its performance, features, and GUIs. For instance, we can update the toolbox to handle branched-chain robots and closed-chain robots. An implicit time integrator can be included to improve the speed of dynamic simulations. We can also include customizable cross sections for the links to simulate a random tube like geometries. Methods can be added to the Linkage class to simulate inverse kinematics and dynamics. As a result, the properties and methods of the toolbox classes may change in future versions. The limitations associated with the toolbox at this stage are that it simulates ideal problems. Simulation cases where external dissipative forces such as friction are critical will see a slight deviation due to the ideal assumption. However, we could add friction models in future editions of the toolbox to tackle this limitation.

As the toolbox is developed in a MATLAB environment, there are plenty of ways to use the output data with the existing MATLAB packages and user-written MATLAB codes. For example, the user can combine the SoRoSim toolbox with an optimization package of MATLAB to develop an optimal robot design for applications. We hope that the users of the SoRoSim toolbox find it user-friendly and will use it for research and engineering applications.

Appendix: Formulae

$$\text{ad}_{\xi(X)} = \begin{pmatrix} \tilde{\mathbf{k}} & \mathbf{0}_{3 \times 3} \\ \tilde{\mathbf{p}} & \tilde{\mathbf{k}} \end{pmatrix} \in \mathbb{R}^{6 \times 6},$$

$$\text{ad}_{\eta(X)} = \begin{pmatrix} \tilde{\mathbf{w}} & \mathbf{0}_{3 \times 3} \\ \tilde{\mathbf{v}} & \tilde{\mathbf{w}} \end{pmatrix} \in \mathbb{R}^{6 \times 6},$$

Adjoint operator of $\mathfrak{se}(3)$.

$$\text{ad}_{\xi(X)}^* = \begin{pmatrix} \tilde{\mathbf{k}} & \tilde{\mathbf{p}} \\ \mathbf{0}_{3 \times 3} & \tilde{\mathbf{k}} \end{pmatrix} \in \mathbb{R}^{6 \times 6},$$

$$\text{ad}_{\eta(X)}^* = \begin{pmatrix} \tilde{\mathbf{w}} & \tilde{\mathbf{v}} \\ \mathbf{0}_{3 \times 3} & \tilde{\mathbf{w}} \end{pmatrix} \in \mathbb{R}^{6 \times 6},$$

Coadjoint operator of $\mathfrak{se}(3)$.

$$\text{Ad}_{g(X)} = \begin{pmatrix} \mathbf{R} & \mathbf{0}_{3 \times 3} \\ \tilde{\mathbf{r}}\mathbf{R} & \mathbf{R} \end{pmatrix} \in \mathbb{R}^{6 \times 6},$$

Adjoint map of $SE(3)$.

$$\text{Ad}_{g(X)}^* = \begin{pmatrix} \mathbf{R} & \tilde{\mathbf{r}}\mathbf{R} \\ \mathbf{0}_{3 \times 3} & \mathbf{R} \end{pmatrix} \in \mathbb{R}^{6 \times 6},$$

Coadjoint map of $SE(3)$.

$$\begin{aligned} \exp(\widehat{\Omega}(X)) &= \mathbf{I}_4 + \widehat{\Omega} + \frac{1}{\theta^2} (1 - \cos(\theta)) \widehat{\Omega}^2 \\ &+ \frac{1}{\theta^3} (\theta - \sin(\theta)) \widehat{\Omega}^3, \end{aligned}$$

Exponential map where θ is the magnitude of Ω .

$$\begin{aligned} \mathbf{T}_\Omega(X) &= \int_0^X \exp(s\text{ad}_\Omega) ds = X\mathbf{I}_6 \\ &+ \frac{1}{2\theta^2} (4 - 4\cos(X\theta) - X\theta\sin(X\theta)) \text{ad}_\Omega \\ &+ \frac{1}{2\theta^3} (4X\theta - 5\sin(X\theta) + X\theta\cos(X\theta)) \text{ad}_\Omega^2 \\ &+ \frac{1}{2\theta^4} (2 - 2\cos(X\theta) - X\theta\sin(X\theta)) \text{ad}_\Omega^3 \\ &+ \frac{1}{2\theta^5} (2X\theta - 3\sin(X\theta) + X\theta\cos(X\theta)) \text{ad}_\Omega^4, \end{aligned}$$

Analytic expression of the tangent operator of the exponential map.

$$\begin{aligned} \dot{\mathbf{T}}_\Omega(X) &= \int_0^X \frac{\partial \exp(s\text{ad}_\Omega)}{\partial t} ds = \\ &\frac{\dot{\theta}}{2\theta^3} (-8 + (8 - X^2\theta^2)\cos(X\theta) + 5X\theta\sin(X\theta)) \text{ad}_\Omega \\ &+ \frac{1}{2\theta^2} (4 - 4\cos(X\theta) - X\theta\sin(X\theta)) (\text{ad}_\Omega) \\ &+ \frac{\dot{\theta}}{2\theta^4} (-8X\theta + (15 - X^2\theta^2)\sin(X\theta) - 7X\theta\cos(X\theta)) \text{ad}_\Omega^2 \\ &+ \frac{1}{2\theta^3} (4X\theta - 5\sin(X\theta) + X\theta\cos(X\theta)) (\text{ad}_\Omega^2) \\ &+ \frac{\dot{\theta}}{2\theta^5} (-8 + (8 - X^2\theta^2)\cos(X\theta) + 5X\theta\sin(X\theta)) \text{ad}_\Omega^3 \\ &+ \frac{1}{2\theta^4} (2 - 2\cos(X\theta) - X\theta\sin(X\theta)) (\text{ad}_\Omega^3) \\ &+ \frac{\dot{\theta}}{2\theta^6} (-8X\theta + (15 - X^2\theta^2)\sin(X\theta) - 7X\theta\cos(X\theta)) \text{ad}_\Omega^4 \\ &+ \frac{1}{2\theta^5} (2X\theta - 3\sin(X\theta) + X\theta\sin(X\theta)) (\text{ad}_\Omega^4), \end{aligned}$$

Analytic expression of the time derivative of the tangent operator of the exponential map.

Acknowledgement

This publication is based upon work supported by the Khalifa University of Science and Technology under Award No. CIRA-2020-074, RC1-2018-KUCARS and Research Excellence (AARE) 2018-05.

Author Disclosure Statement

The authors declare no competing interests.

References

¹ C. Laschi, B. Mazzolai, and M. Cianchetti, “Soft robotics: Technologies and systems pushing the boundaries of robot abilities,” *Science Robotics*, vol. 1, no. 1, 2016.

² R. J. Webster and B. A. Jones, “Design and kinematic modeling of constant curvature continuum robots: A review,” *The International Journal of Robotics Research*, vol. 29, no. 13, pp. 1661–1683, 2010.

³ J. Burgner-Kahrs, D. C. Rucker, and H. Choset, “Continuum robots for medical applications: A survey,” *IEEE Transactions on Robotics*, vol. 31, no. 6, pp. 1261–1280, 2015.

⁴ M. Thieffry, A. Kruszewski, C. Duriez, and T. Guerra, “Control design for soft robots based on reduced-order model,” *IEEE Robotics and Automation Letters*, vol. 4, pp. 25–32, Jan 2019.

⁵ D. Holland, S. Berndt, M. Herman, and C. Walsh, “Growing the soft robotics community through knowledge-sharing initiatives,” *Soft Robotics*, vol. 5, no. 2, pp. 119–121, 2018.

⁶ M. A. Graule, C. B. Teeple, T. P. McCarthy, R. C. St. Louis, G. R. Kim, and R. J. Wood, “Somo: Fast and accurate simulations of continuum robots in complex environments,” in *2021 IEEE International Conference on Intelligent Robots and Systems (IROS)*, p. In Review, IEEE, 2021.

⁷ E. Coevoet, T. Morales-Bieze, F. Largilliere, Z. Zhang, M. Thieffry, M. Sanz-Lopez, B. Carrez, D. Marchal, O. Goury, J. Dequidt, *et al.*, “Software toolkit for modeling, simulation, and control of soft robots,” *Advanced Robotics*, vol. 31, no. 22, pp. 1208–1224, 2017.

⁸ F. Faure, C. Duriez, H. Delingette, J. Allard, B. Gilles, S. Marchesseau, H. Talbot, H. Courtecuisse, G. Bousquet, I. Peterlik, and S. Cotin, “SOFA: A Multi-Model Framework for Interactive Physical Simulation,” in *Soft Tissue Biomechanical Modeling for Computer Assisted Surgery* (Y. Payan, ed.), vol. 11 of *Studies in Mechanobiology, Tissue Engineering and Biomaterials*, pp. 283–321, Springer, June 2012.

⁹ N. Naughton, J. Sun, A. Tekinalp, T. Parthasarathy, G. Chowdhary, and M. Gazzola, “Elastica: A compliant mechanics environment for soft robotic control,” *IEEE*

Robotics and Automation Letters, vol. 6, no. 2, pp. 3389–3396, 2021.

¹⁰ B. Angles, D. Rebain, M. Macklin, B. Wyvill, L. Barthe, J. Lewis, J. Von Der Pahlen, S. Izadi, J. Valentin, S. Bouaziz, *et al.*, “Viper: Volume invariant position-based elastic rods,” *Proceedings of the ACM on Computer Graphics and Interactive Techniques*, vol. 2, no. 2, pp. 1–26, 2019.

¹¹ S. H. Sadati, S. E. Naghibi, A. Shiva, B. Michael, L. Renson, M. Howard, C. D. Rucker, K. Althoefer, T. Nanayakkara, S. Zschaler, *et al.*, “Tmtdyn: A matlab package for modeling and control of hybrid rigid–continuum robots based on discretized lumped systems and reduced-order models,” *The International Journal of Robotics Research*, vol. 40, no. 1, pp. 296–347, 2021.

¹² F. Renda, C. Armanini, V. Lebastard, F. Candelier, and F. Boyer, “A geometric variable-strain approach for static modeling of soft manipulators with tendon and fluidic actuation,” *IEEE Robotics and Automation Letters*, vol. 5, no. 3, pp. 4006–4013, 2020.

¹³ F. Boyer, V. Lebastard, F. Candelier, and F. Renda, “Dynamics of continuum and soft robots: A strain parameterization based approach,” *IEEE Transactions on Robotics*, pp. 1–17, 2020.

¹⁴ “Optimization toolbox: Solve linear, quadratic, conic, integer, and nonlinear optimization problems.” <https://www.mathworks.com/products/optimization.html>.

¹⁵ “Control system toolbox: Design and analyze control systems.” <https://www.mathworks.com/products/control.html>.

¹⁶ R. Murray, Z. Li, and S. Sastry, *A Mathematical Introduction to Robotic Manipulation*. Taylor & Francis, Boca Raton, USA, 1994.

¹⁷ F. Renda and L. Seneviratne, “A geometric and unified approach for modeling soft-rigid multi-body systems with lumped and distributed degrees of freedom,” in *2018 IEEE International Conference on Robotics and Automation (ICRA)*, pp. 1567–1574, May 2018.

¹⁸ E. Hairer, C. Lubich, and G. Wanner, *Geometric Numerical Integration: Structure-Preserving Algorithms for Ordinary Differential Equations*. Springer series in computational mathematics, Springer, 2006.

¹⁹ J. Selig, *Geometric Fundamentals of Robotics*. Monographs in Computer Science, Springer New York, 2007.

²⁰ F. Boyer and F. Renda, “Poincare’s equations for cosserat media: Application to shells,” *Journal of Nonlinear Science*, vol. 27, no. 1, pp. 1–44, 2017.

²¹ R. Featherstone, *Rigid Body Dynamics Algorithms*. Springer New York, 2008.

²² F. Renda, M. Cianchetti, H. Abidi, J. Dias, and L. Seneviratne, “Screw-based modeling of soft manipulators with tendon and fluidic actuation,” *Journal of Mechanism and Robotics*, 2017. doi:10.1115/1.4036579.

²³ F. Renda, F. Boyer, J. Dias, and L. Seneviratne, “Discrete cosserat approach for multisection soft manipulator dynamics,” *IEEE Transactions on Robotics*, vol. 34, pp. 1518–1533, Dec 2018.

²⁴ C. Armanini, I. Hussain, M. Z. Iqbal, D. Gan, D. Prattichizzo, and F. Renda, “Discrete cosserat approach for closed-chain soft robots: Application to the fin-ray finger,” *IEEE Transactions on Robotics*, pp. 1–10, 2021.

²⁵ F. Renda, V. Cacucciolo, J. Dias, and L. Seneviratne, “Discrete cosserat approach for soft robot dynamics: A new piece-wise constant strain model with torsion and shears,” in *2016 IEEE/RSJ International Conference on Intelligent Robots and Systems (IROS)*, pp. 5495–5502, Oct 2016.

²⁶ A. Zanna, “Collocation and relaxed collocation for the fer and the magnus expansions,” *SIAM J. Numer. Anal.*, vol. 36, pp. 1145–1182, Apr. 1999.

²⁷ A. L. Orekhov and N. Simaan, “Solving cosserat rod models via collocation and the

magnus expansion,” in *2020 IEEE/RSJ International Conference on Intelligent Robots and Systems (IROS)*, pp. 8653–8660, 2020.

²⁸ G. Blaschek, “Principles of object-oriented programming,” in *Object-Oriented Programming*, pp. 9–90, Springer, 1994.

²⁹ “Sorosim: An open-chain robotics simulation toolbox.” <https://www.mathworks.com/matlabcentral/fileexchange/83038-sorosim>. Version 2.32, Updated 11 Jul 2021.

³⁰ F. Boyer and D. Primault, “Finite element of slender beams in finite transformations: a geometrically exact approach,” *International Journal for Numerical Methods in Engineering*, vol. 59, no. 5, pp. 669–702, 2004.

³¹ M. Calisti, F. Giorgio-Serchi, C. Stefanini, M. Farman, I. Hussain, C. Armanini, D. Gan, L. Seneviratne, and F. Renda, “Design, modeling and testing of a flagellum-inspired soft underwater propeller exploiting passive elasticity,” in *2019 IEEE/RSJ International Conference on Intelligent Robots and Systems (IROS)*, pp. 3328–3334, 2019.

³² C. Armanini, M. Farman, M. Calisti, F. Giorgio-Serchi, C. Stefanini, and F. Renda, “Flagellate underwater robotics at macro-scale: Design, modeling and characterization,” *IEEE Transaction on Robotics*. In press.

³³ A. T. Mathew, I. Hussain, C. Stefanini, I. M. B. Hmida, and F. Renda, “Resoft gripper: A reconfigurable soft gripper with monolithic fingers and differential mechanism for versatile and delicate grasping,” in *2021 4th IEEE International Conference on Soft Robotics (RoBoSoft)*, p. Accepted, IEEE, 2021.

Correspondence Address

Federico Renda,
Department of Mechanical Engineering, Khalifa University of Science and Technology, Abu Dhabi, UAE and Khalifa University Center for Autonomous Robotic Systems (KUCARS), Khalifa University, Abu Dhabi, UAE.
federico.renda@ku.ac.ae.

List of Figures

1	Schematics of the proposed kinematics for a floating hybrid soft/rigid chain.	21
2	Schematics of the dynamics of a soft link internally actuated.	22
3	Graphical representation of the two-level nested quadrature scheme for a soft link i . In this particular example, three points are used for the Gauss quadrature (forth-order) and 2 points are used for the Zanna's collocation method (forth-order).	23
4	Steps for creating a soft link with a fixed joint, circular cross section, and 2 divisions ($1 \rightarrow 2 \rightarrow 3 \rightarrow 4$) and a rigid link with a revolute joint and rectangular cross section ($1 \rightarrow 2 \rightarrow 3$).	24
5	Steps for obtaining the Twist class elements during the Linkage class creation ($1 \rightarrow 2 \rightarrow 3 \rightarrow 4$). Dialog boxes will appear for each piece, from the start to the end of the linkage. The GUI will highlight the corresponding piece at the same time. The numbers shown on the linkage image corresponds to the piece numbers. Red, green, and blue arrows indicate x, y, and z axes, respectively.	25
6	Steps for obtaining the External Force Properties of the Linkage class ($1 \rightarrow 2 \rightarrow 3 \rightarrow 4 \rightarrow 5$). Dialog boxes will appear for applying gravity, followed by point wrenches. . . .	26
7	Steps for obtaining the Actuation Properties associated with the rigid joints of the Linkage class ($1 \rightarrow 2 \rightarrow 3$).	27
8	Steps for obtaining the Actuation Properties of soft links of the Linkage class ($4 \rightarrow 5 \rightarrow 6 \rightarrow 7 \rightarrow 8 \rightarrow 9$).	28
9	Step for entering the stiffness value of revolute and prismatic joints and the final image of the linkage.	29
10	The static equilibrium state of the linkage when the revolute joint angle (θ) is $-\pi/2$ and the cable tension is 200 N. The reference configuration and the equilibrium state of the Linkage when $\theta = 0$ and $T = 0N$ are also plotted for comparison.	30
11	The states of the linkage at different times of the dynamic simulation ($t=0s, 0.125s, 0.25s, 0.375s, 0.5s, 0.75s, 1s$, and $2s$) when the revolute joint angle, $\theta = (\pi/2)\sin(2\pi t)$ and the cable tension is a ramp input that reaches 200 N at 1 second and stays at 200 N after 1 second. The trajectory of the tip of the rigid link during the time, $t=0$ to $1s$ is indicated as a green dashed line.	31
12	Rod deflection plots under follower tip forces varying from 0 to 130 kN	32
13	Plots showing the motion and the energy balance of the undamped rod and undamped rod as they falls due to gravity: (a) Superimposed images of the damped case. (b) Superimposed images of the undamped case. The dashed line shows the tip trajectory. (c) Energy plot of the undamped and damped free fall. The dashed and the solid lines represent the undamped and the damped cases.	33
14	(a) Path of the cable within the soft link. (b) Static equilibrium when the cable tension is 250 N.	34
15	Plots showing the path of the soft rod as it approaches the desired location (green box) while avoiding an obstacle (red box) with the help of multiple actuation cables. The dashed line shows the path the soft link tip follows as the link moves.	35
16	Motion of the flagellate robot between $t=0s$ and $3.5s$ due to the thrust force generated by the soft propeller. The dotted line in the figure shows the path that the tip of the soft filament follows as the robot moves.	36
17	Motion of an under-actuated open chain hybrid linkage between $t = 0s$ and $1.5s$. The dashed line shows the tip trajectory of the soft link as the revolute joint rotate with an angular velocity of π rad/s.	37
18	(a) Image of the ReSoft gripper from. ³³ (b) Equilibrium state of the gripper when the cable tension is 2.5N, and the revolute joint angle is $0^\circ, 120^\circ$ (Tripod), and 180°	38

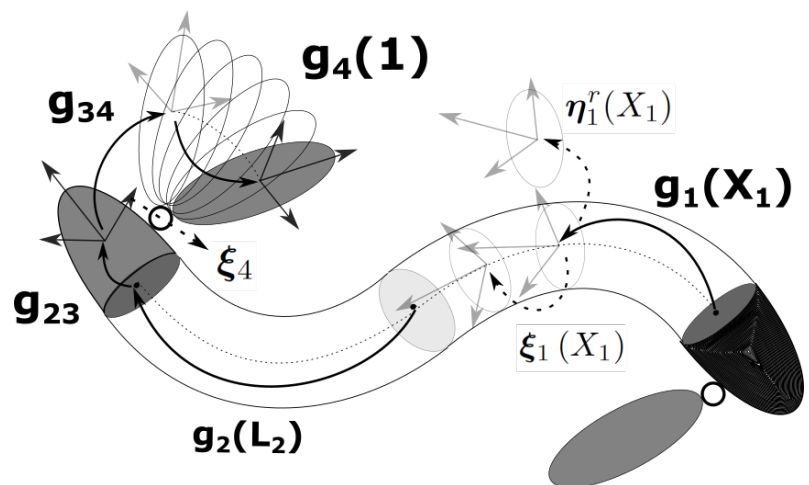


Figure 1. Schematics of the proposed kinematics for a floating hybrid soft/rigid chain.

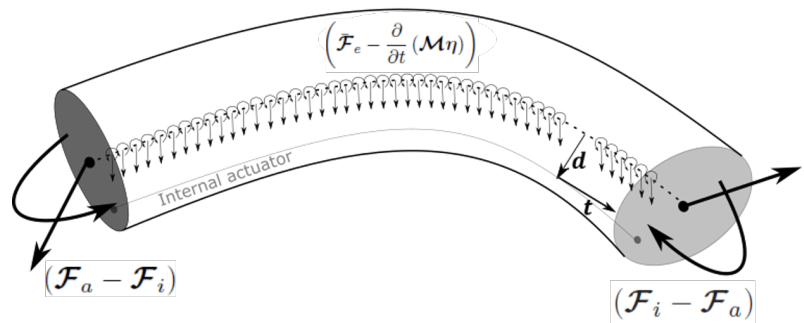


Figure 2. Schematics of the dynamics of a soft link internally actuated.

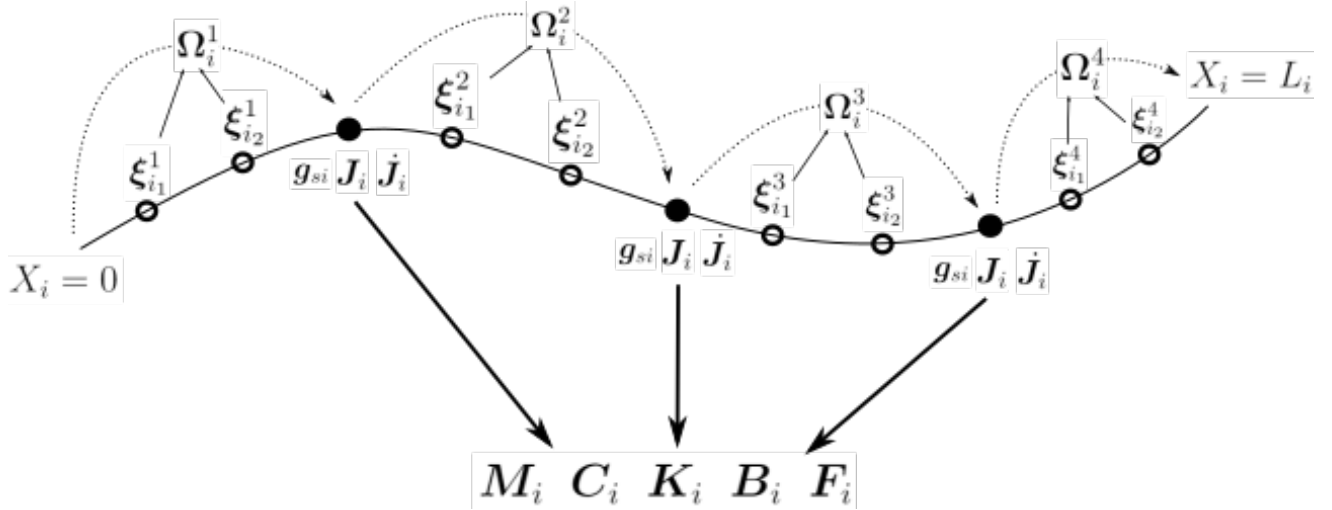


Figure 3. Graphical representation of the two-level nested quadrature scheme for a soft link i . In this particular example, three points are used for the Gauss quadrature (forth-order) and 2 points are used for the Zanna's collocation method (forth-order).

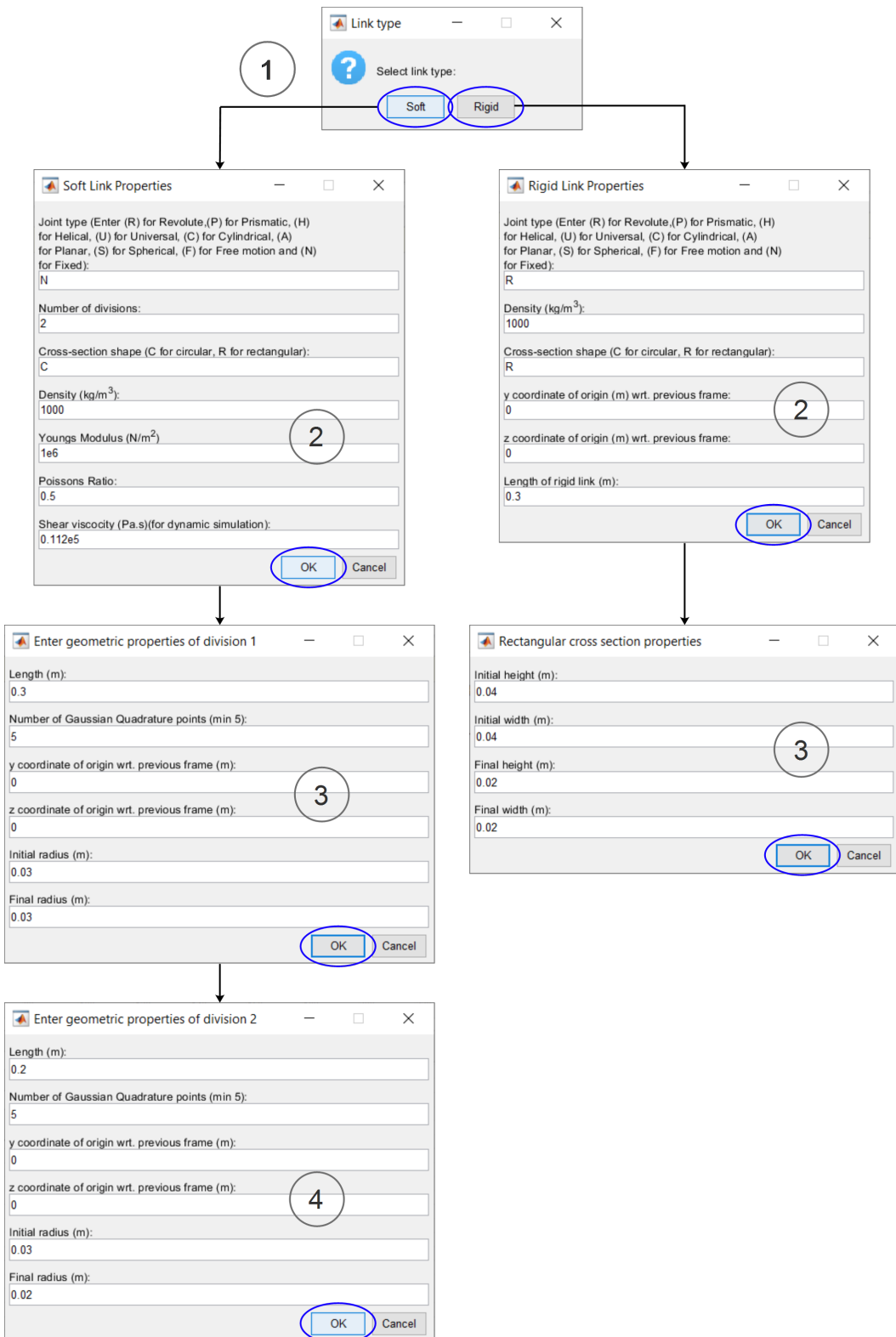


Figure 4. Steps for creating a soft link with a fixed joint, circular cross section, and 2 divisions (1 → 2 → 3 → 4) and a rigid link with a revolute joint and rectangular cross section (1 → 2 → 3).

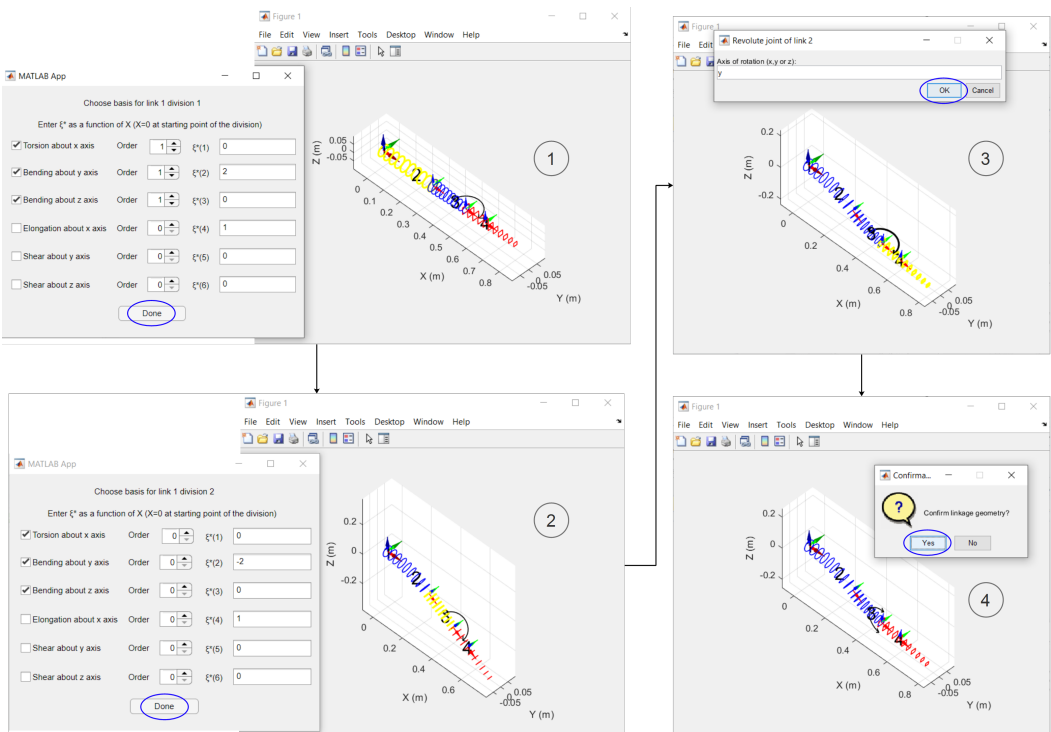


Figure 5. Steps for obtaining the Twist class elements during the Linkage class creation (1→2→3→4). Dialog boxes will appear for each piece, from the start to the end of the linkage. The GUI will highlight the corresponding piece at the same time. The numbers shown on the linkage image corresponds to the piece numbers. Red, green, and blue arrows indicate x, y, and z axes, respectively.

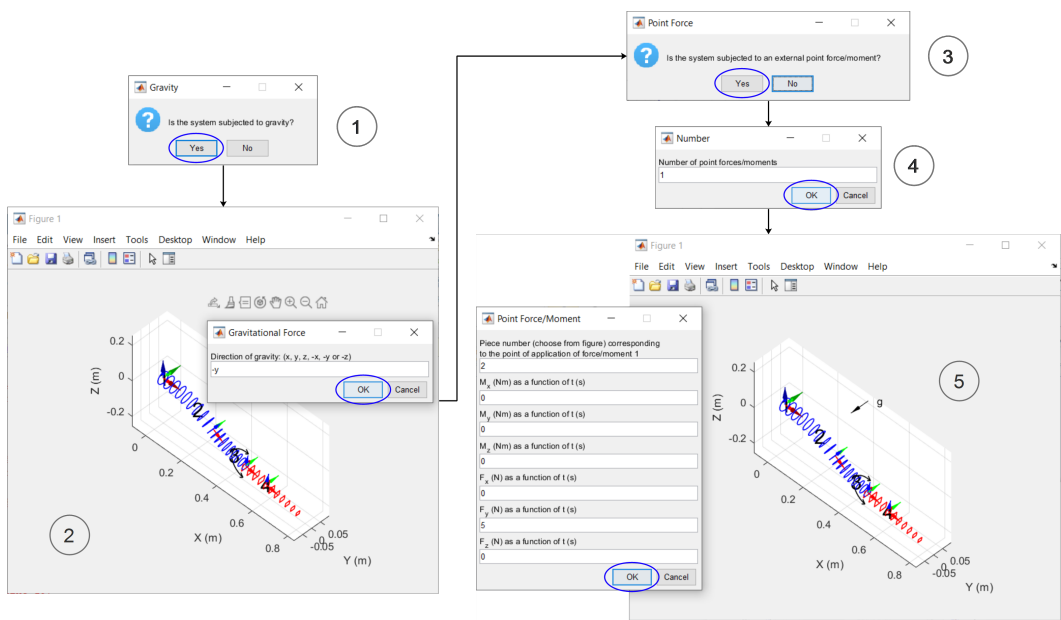


Figure 6. Steps for obtaining the External Force Properties of the Linkage class (1→2→3→4→5). Dialog boxes will appear for applying gravity, followed by point wrenches.

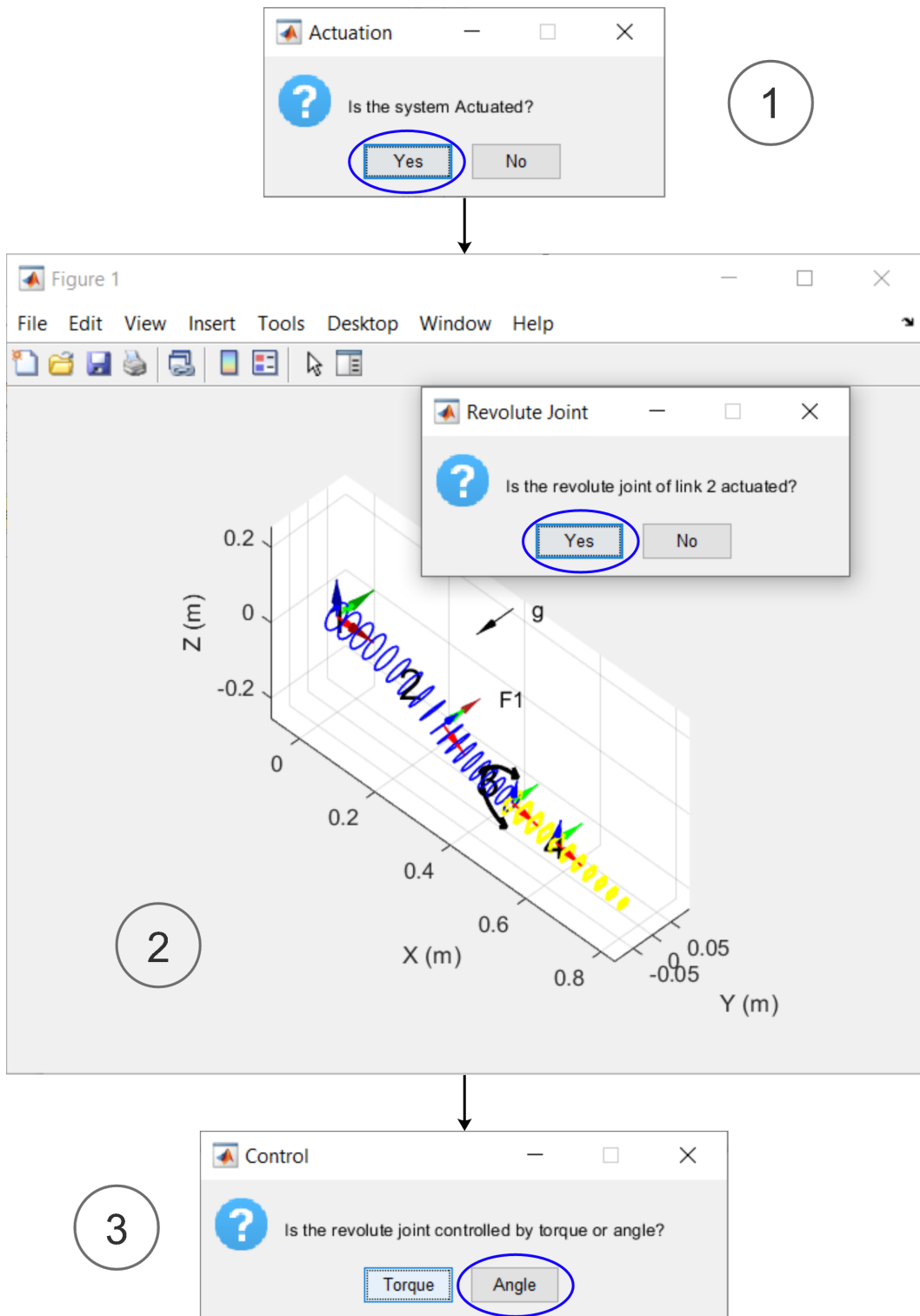


Figure 7. Steps for obtaining the Actuation Properties associated with the rigid joints of the Linkage class (1→2→3).

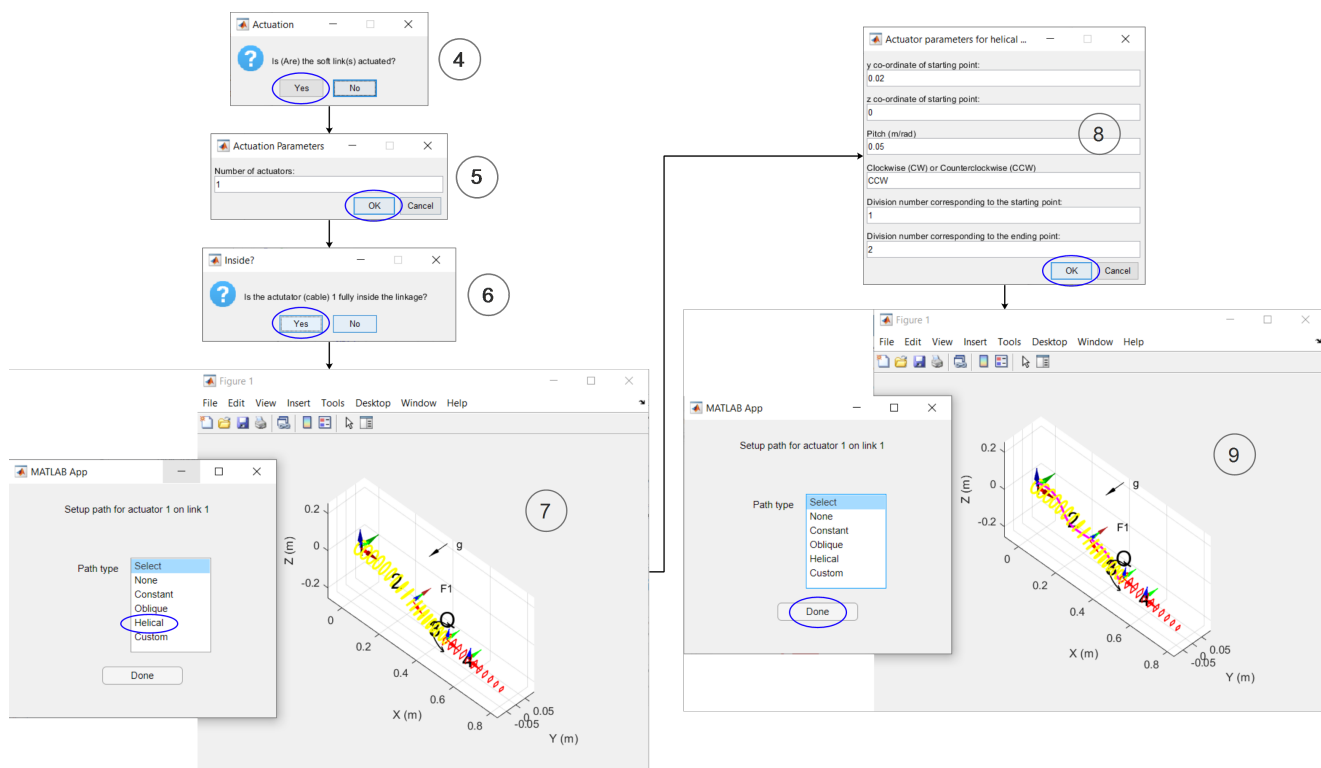


Figure 8. Steps for obtaining the Actuation Properties of soft links of the Linkage class (4 → 5 → 6 → 7 → 8 → 9).

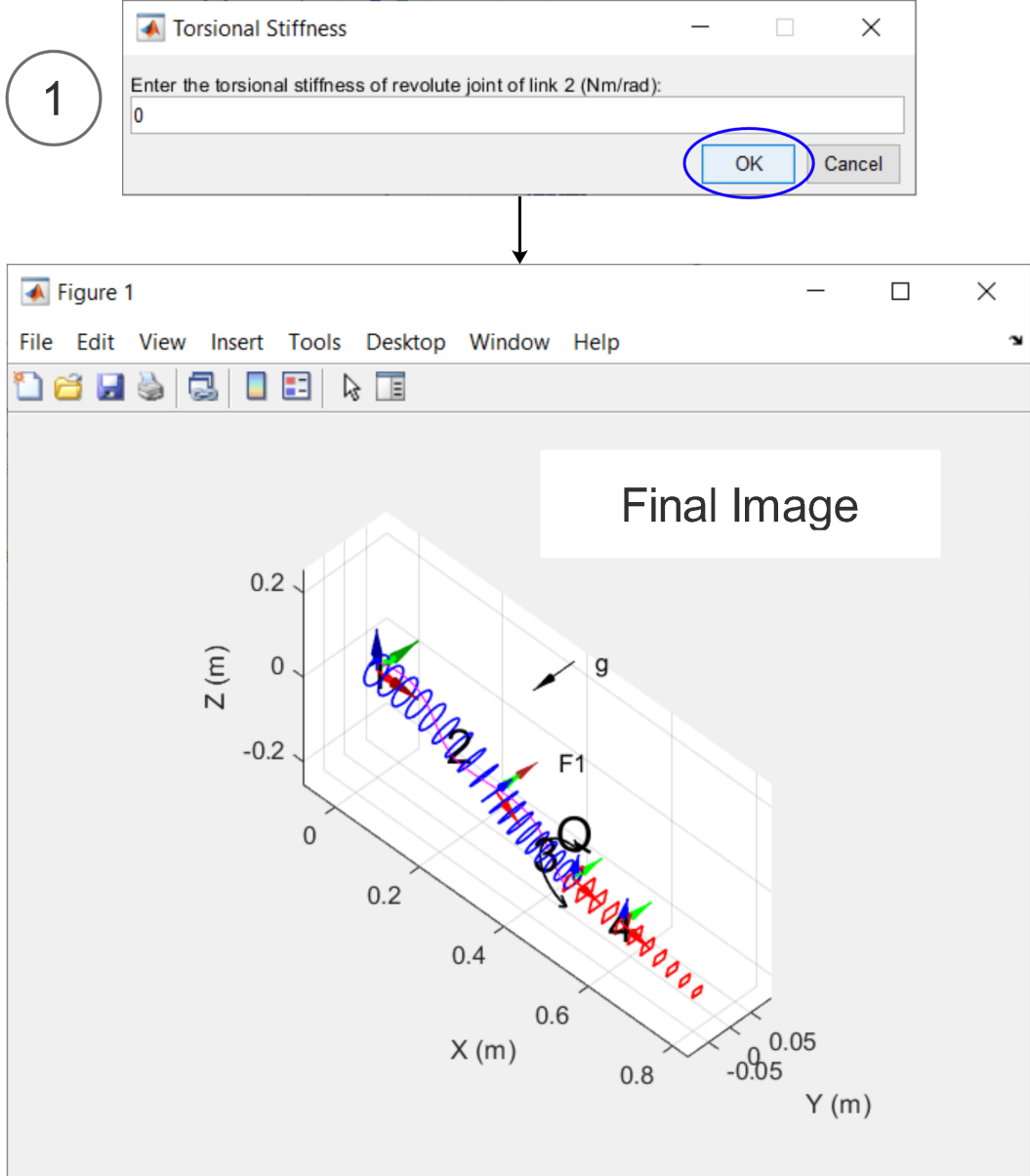


Figure 9. Step for entering the stiffness value of revolute and prismatic joints and the final image of the linkage.

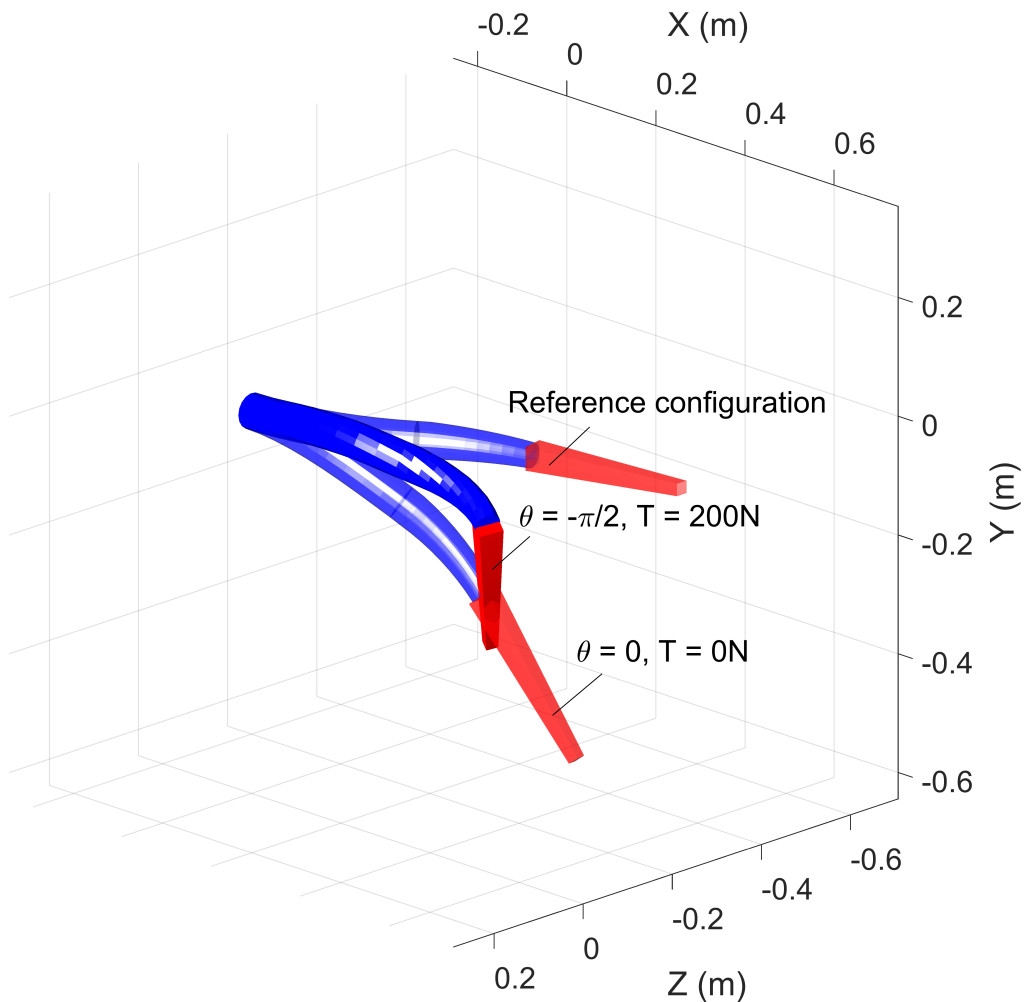


Figure 10. The static equilibrium state of the linkage when the revolute joint angle (θ) is $-\pi/2$ and the cable tension is 200 N. The reference configuration and the equilibrium state of the Linkage when $\theta = 0$ and $T = 0N$ are also plotted for comparison.

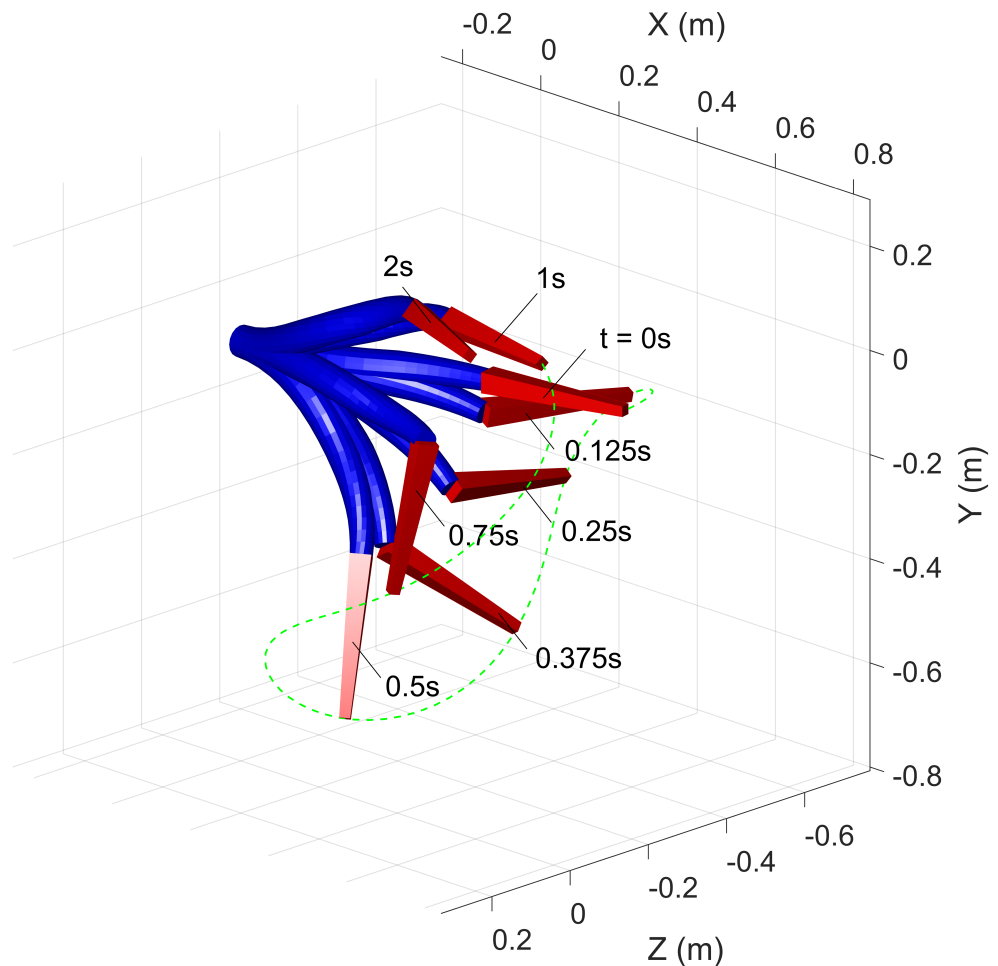


Figure 11. The states of the linkage at different times of the dynamic simulation ($t=0s, 0.125s, 0.25s, 0.375s, 0.5s, 0.75s, 1s$, and $2s$) when the revolute joint angle, $\theta = (\pi/2)\sin(2\pi t)$ and the cable tension is a ramp input that reaches 200 N at 1 second and stays at 200 N after 1 second. The trajectory of the tip of the rigid link during the time, $t=0$ to $1s$ is indicated as a green dashed line.

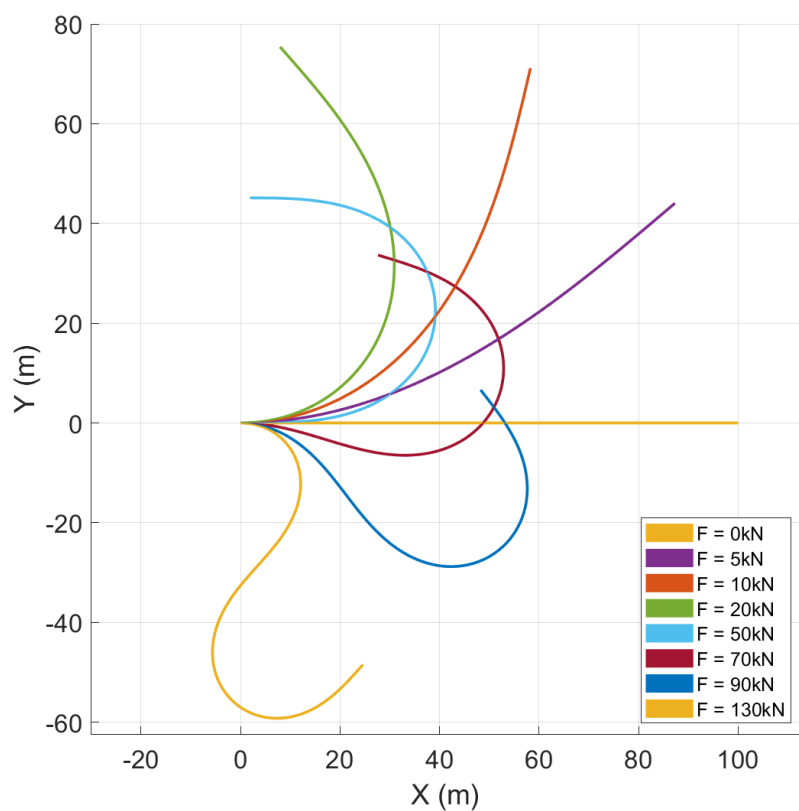


Figure 12. Rod deflection plots under follower tip forces varying from 0 to 130 kN

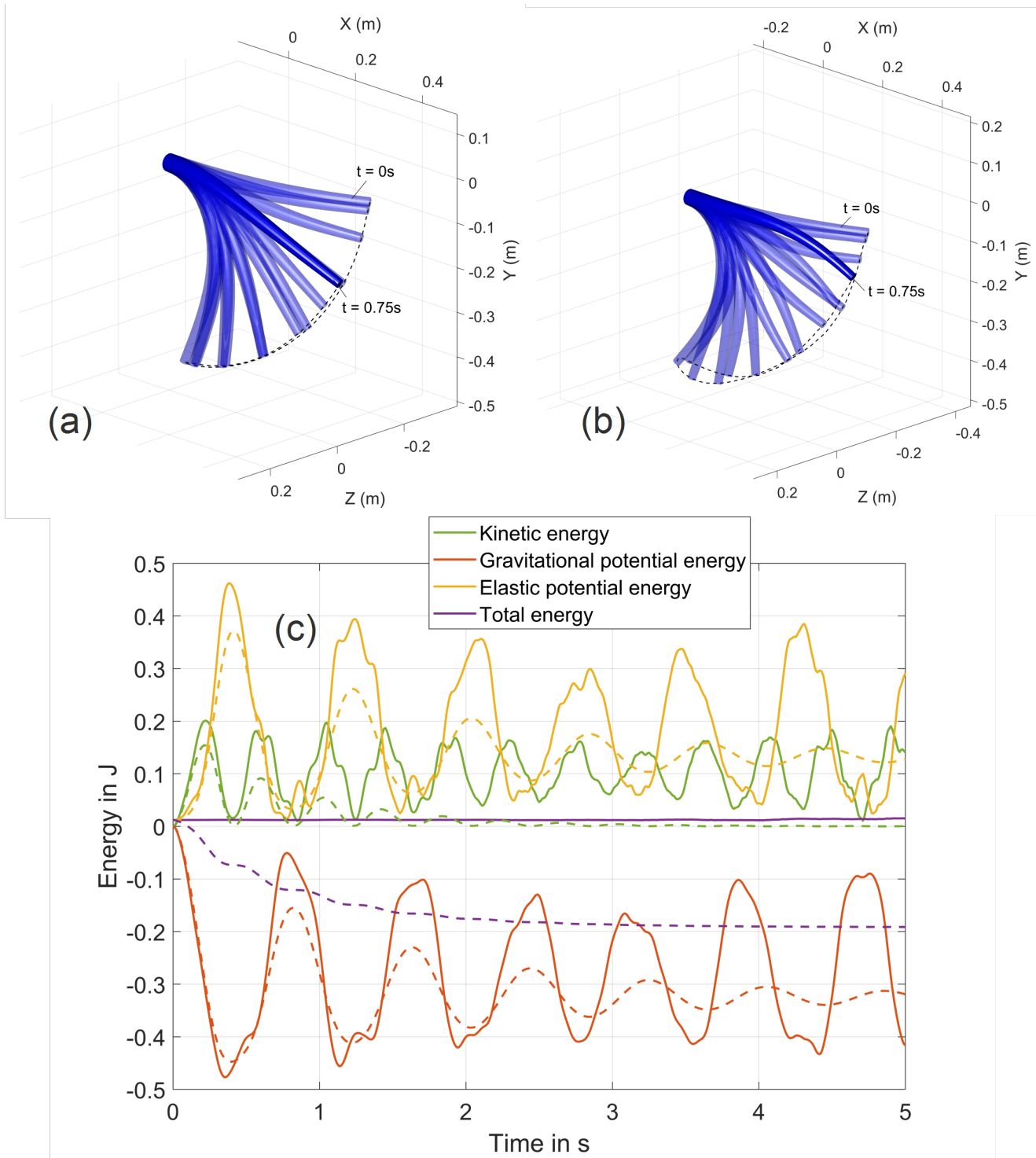


Figure 13. Plots showing the motion and the energy balance of the undamped rod and undamped rod as they falls due to gravity: (a) Superimposed images of the damped case. (b) Superimposed images of the undamped case. The dashed line shows the tip trajectory. (c) Energy plot of the undamped and damped free fall. The dashed and the solid lines represent the undamped and the damped cases.

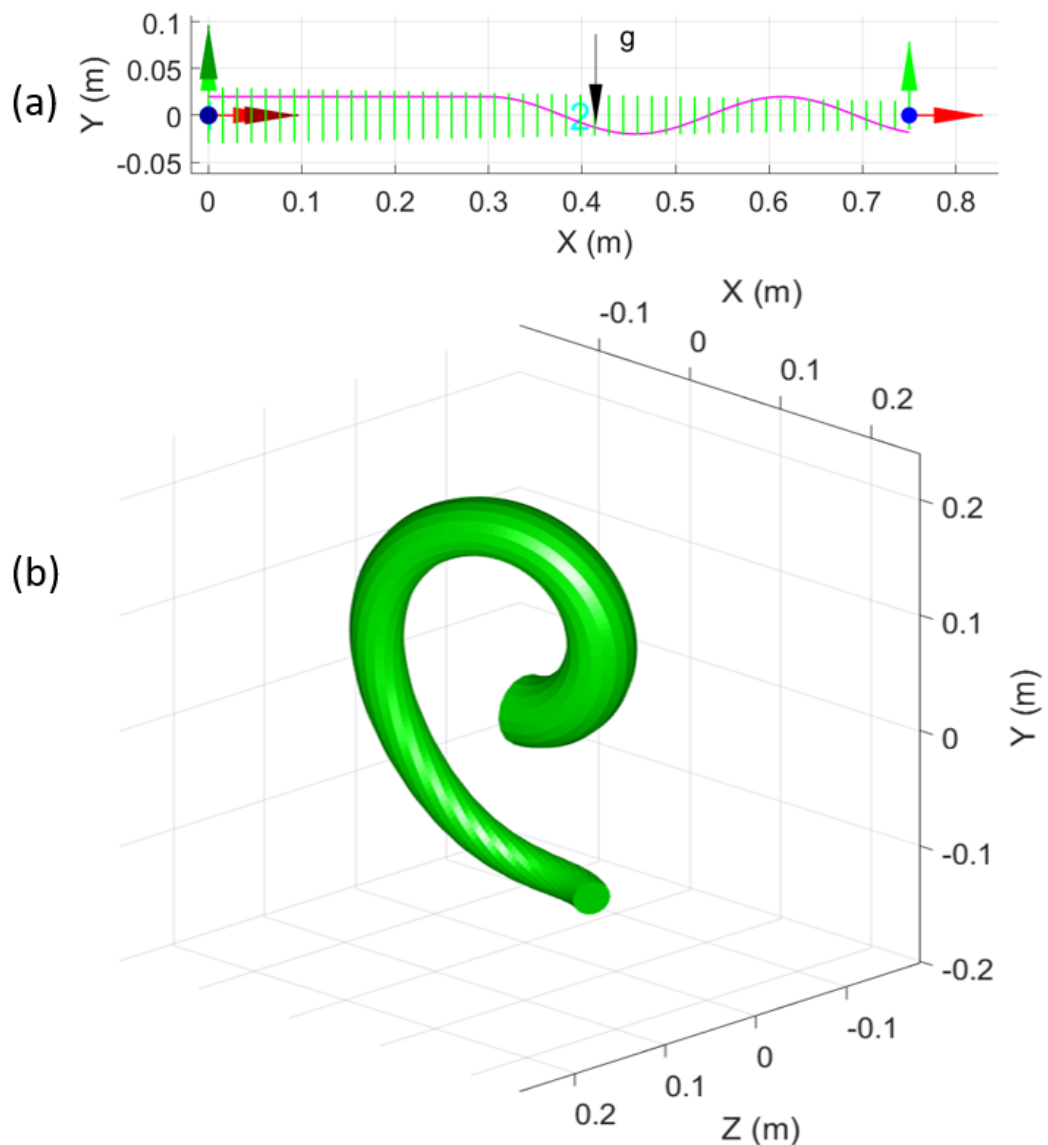


Figure 14. (a) Path of the cable within the soft link. (b) Static equilibrium when the cable tension is 250 N.

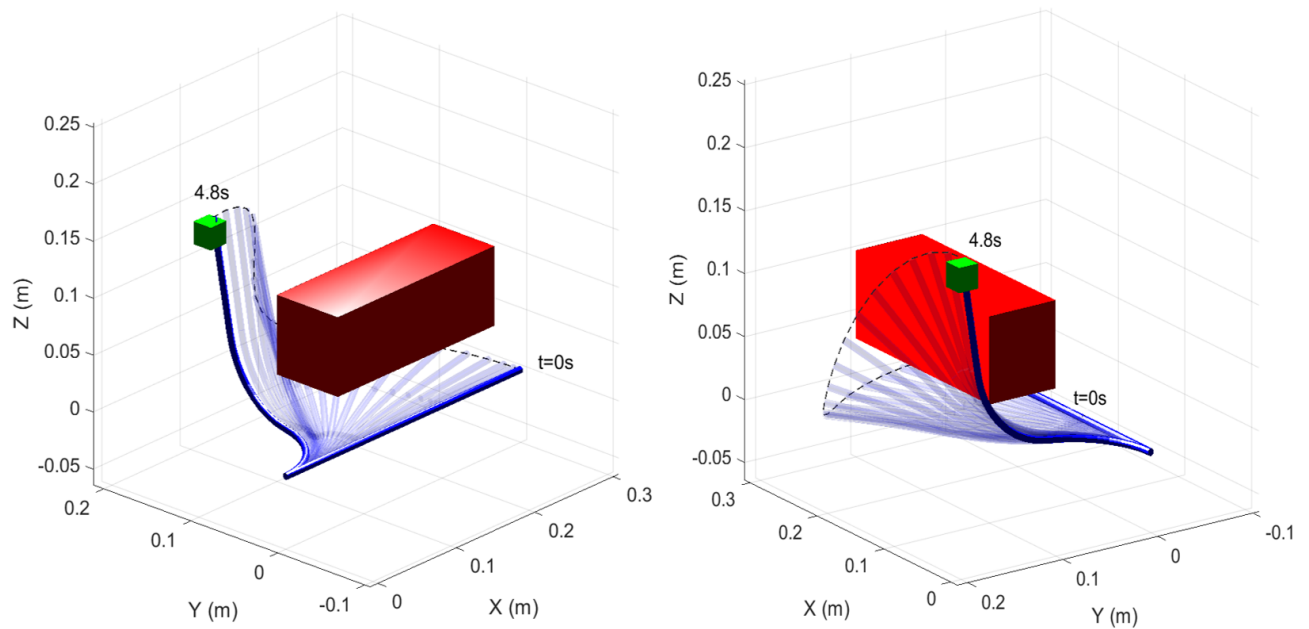


Figure 15. Plots showing the path of the soft rod as it approaches the desired location (green box) while avoiding an obstacle (red box) with the help of multiple actuation cables. The dashed line shows the path the soft link tip follows as the link moves.

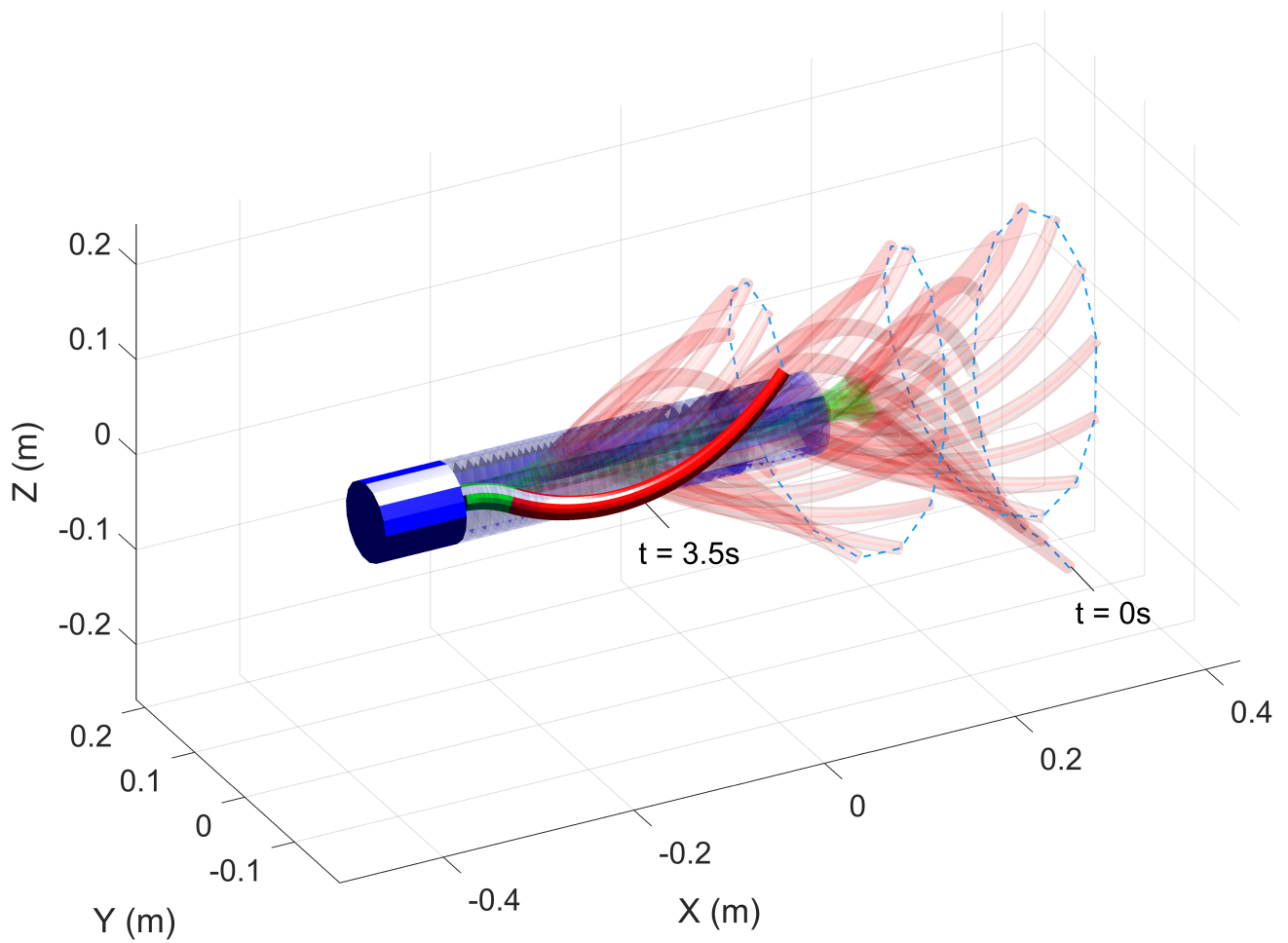


Figure 16. Motion of the flagellate robot between $t=0s$ and $3.5s$ due to the thrust force generated by the soft propeller. The dotted line in the figure shows the path that the tip of the soft filament follows as the robot moves.

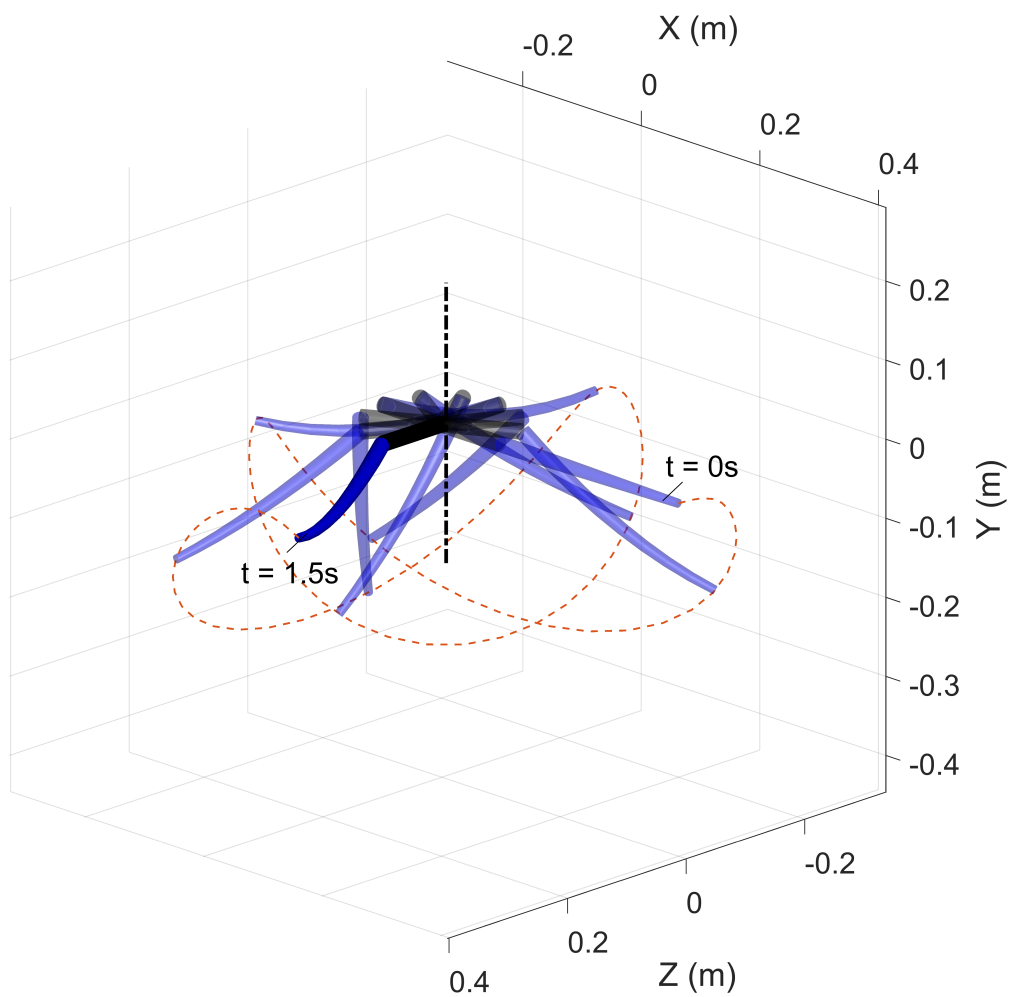


Figure 17. Motion of an under-actuated open chain hybrid linkage between $t = 0s$ and $1.5s$. The dashed line shows the tip trajectory of the soft link as the revolute joint rotate with an angular velocity of π rad/s.

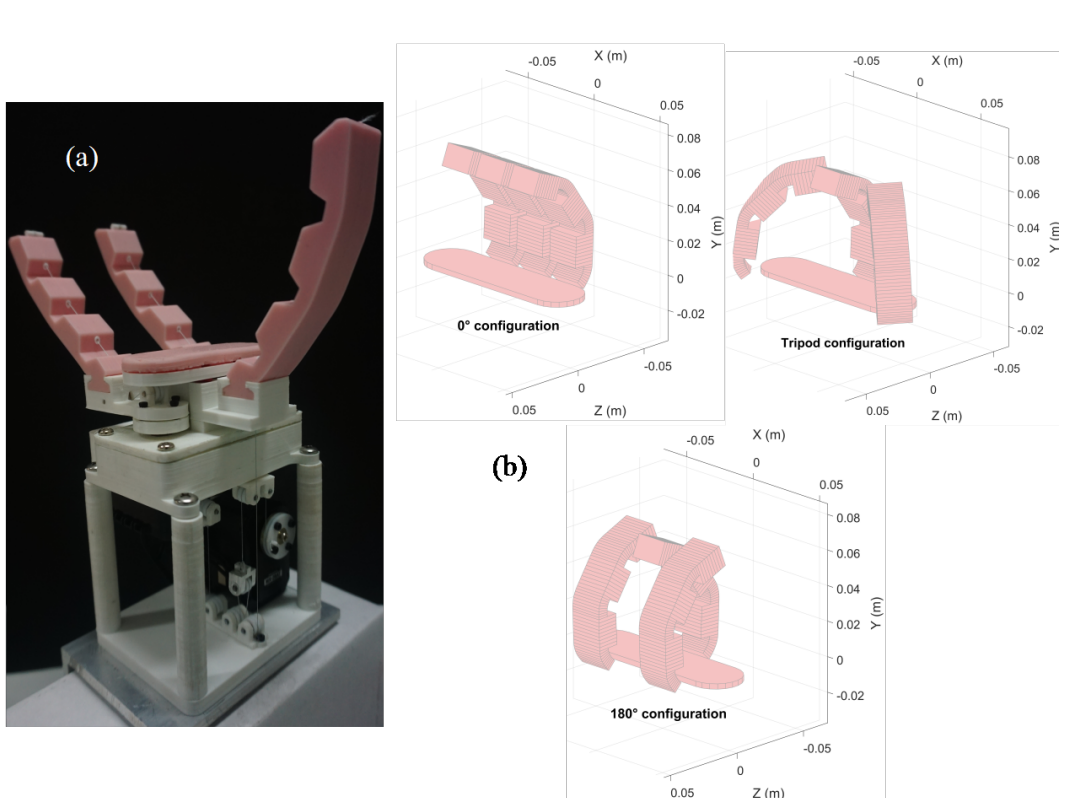


Figure 18. (a) Image of the ReSoft gripper from.³³ (b) Equilibrium state of the gripper when the cable tension is 2.5N, and the revolute joint angle is 0°, 120° (Tripod), and 180°

List of Tables

1	Properties of Link Class	40
2	Examples of base matrices of lumped joints	41
3	Examples of base matrices of distributed joints (soft piece). N_1 , N_2 , N_3 , and N_4 are orders of polynomials used to fit the strains associated with different deformation modes. The generalized force ((τ_i)) of a distributed joint is given by, $\int_0^{L_i} \mathbf{B}_{\xi_i}^T \mathcal{F}_{a_i} dX_i$	42
4	Properties of Twist Class	43
5	Properties of Linkage Class	44
6	Methods of the Linkage Class. S is the name of the Linkage.	45

Type	Name	Description
General Properties	jointtype	Jointtype of the link: 'R' for revolute, 'P' for prismatic, 'H' for helical, 'U' for universal, 'C' for cylindrical, 'A' for planar, 'S' for spherical, 'F' for free motion, and 'N', for fixed joint
	linktype	Type of link: 's' for soft body, 'r' for rigid body
	CS	Cross sectional shape: 'C' for circular and 'R' for rectangular
	npie	1 for rigid link and 1+number of divisions for soft link
	nGauss	Cell element with of number of Gauss quadrature points for each division (including the start and end point) of a soft link
	Xs	Cell element of corresponding Gauss quadrature points computed between 0 and 1
Geometric Properties	Ws	Cell element of corresponding weights
	lp	Cell element of piece-wise lengths of each divisions of the soft link [m]
	L	Total length of the link [m]
	r	Radius of the rigid link or cell element of the same for all divisions of the soft link. Saved as a function of $X1 = X/L$ for rigid link or $X1 = X/lp\{division_number\}$ for soft divisions [m]
	h	Height of the rigid link or cell element of the same for all divisions of the soft link (as a function of X1) [m]
	w	Width of the rigid link or cell element of the same for all divisions of the soft link (as a function of X1)[m]
Material Properties	cx, cy, cz	Coordinates of origin with respect to previous frame for the rigid link or cell element of the same for all divisions of the soft link [m]
	E, Poi, G,	Young's modulus [Pa], Poisson's ratio [-], shear modulus [Pa], and material damping [Pa.s] of the soft link
	Eta	Density of the link [kg/m^3]
	Rho	Screw inertial matrix of the rigid link or cell element of cross sectional screw inertial matrix for all divisions of the soft link
	Ms	Cell element of cross sectional screw stiffness matrix for all divisions of the soft link
	Es	Cell element of cross sectional screw damping matrix for all divisions of the soft link
	Gs	Cell element of cross sectional screw damping matrix for all divisions of the soft link

Table 1. Properties of Link Class

DoF	Joint	Base (\mathbf{B})	Generalized Force (τ_i)
0	Fixed	-	-
1	Revolute (about x axis)	$\begin{bmatrix} 1 \\ 0 \\ 0 \\ 0 \\ 0 \\ 0 \end{bmatrix}, \begin{bmatrix} 0 \\ 0 \\ 0 \\ 1 \\ 0 \\ 0 \end{bmatrix}, \begin{bmatrix} 1 \\ 0 \\ 0 \\ p \\ 0 \\ 0 \end{bmatrix}$	$\mathbf{B}_{\xi_i}^T \mathcal{F}_{J_i}$
	Prismatic (along x axis)		
	Helical (along x axis)		
2	Universal (constrained about x axis)	$\begin{bmatrix} 0 \\ 1 \\ 0 \\ 0 \\ 0 \\ 0 \end{bmatrix} \& \begin{bmatrix} 0 \\ 0 \\ 1 \\ 0 \\ 0 \\ 0 \end{bmatrix}$	$\mathbf{B}_{\xi_i}^T \mathcal{F}_{J_i}$
	Cylindrical (about x axis)	$\begin{bmatrix} 0 & 0 & 0 \\ 0 & 0 & 0 \\ 1 & 0 & 0 \\ 0 & 1 & 0 \\ 0 & 0 & 0 \\ 0 & 0 & 0 \end{bmatrix}$	${}^i \mathbf{S}_i^T \mathcal{F}_{J_i}$
3	Planar (x-y plane)	$\begin{bmatrix} 0 & 0 & 0 \\ 0 & 0 & 0 \\ 1 & 0 & 0 \\ 0 & 1 & 0 \\ 0 & 0 & 1 \\ 0 & 0 & 0 \end{bmatrix}$	${}^i \mathbf{S}_i^T \mathcal{F}_{J_i}$
	Spherical	$\begin{bmatrix} 1 & 0 & 0 \\ 0 & 1 & 0 \\ 0 & 0 & 1 \\ 0 & 0 & 0 \\ 0 & 0 & 0 \\ 0 & 0 & 0 \end{bmatrix}$	${}^i \mathbf{S}_i^T \mathcal{F}_{J_i}$
6	Free Motion	\mathbf{I}_6	${}^i \mathbf{S}_i^T \mathcal{F}_{J_i}$

Table 2. Examples of base matrices of lumped joints

Beam	Base (\mathbf{B})	DoF
Linear Spring	$\begin{bmatrix} 0 & 0 & \dots & 0 \\ 0 & 0 & \dots & 0 \\ 0 & 0 & \dots & 0 \\ 1 & X & \dots & X^{N_4} \\ 0 & 0 & \dots & 0 \\ 0 & 0 & \dots & 0 \end{bmatrix}$	$N_4 + 1$
Planar Constant Curvature	$\begin{bmatrix} 0 & 0 & \dots & 0 & 0 & 0 & \dots & 0 \\ 0 & 0 & \dots & 0 & 0 & 0 & \dots & 0 \\ 1 & X & \dots & X^{N_3} & 0 & 0 & \dots & 0 \\ 0 & 0 & \dots & 0 & 1 & X & \dots & X^{N_4} \\ 0 & 0 & \dots & 0 & 0 & 0 & \dots & 0 \\ 0 & 0 & \dots & 0 & 0 & 0 & \dots & 0 \\ 0 & 0 & \dots & 0 & 0 & 0 & \dots & 0 \end{bmatrix}$	$N_3 + N_4 + 2$
Inextensible Constant Curvature	$\begin{bmatrix} 1 & X & \dots & X^{N_1} & 0 & 0 & \dots & 0 & 0 & 0 & \dots & 0 \\ 0 & 0 & \dots & 0 & 1 & X & \dots & X^{N_2} & 0 & 0 & \dots & 0 \\ 0 & 0 & \dots & 0 & 0 & 0 & \dots & 0 & 1 & X & \dots & X^{N_3} \\ 0 & 0 & \dots & 0 & 0 & 0 & \dots & 0 & 0 & 0 & \dots & 0 \\ 0 & 0 & \dots & 0 & 0 & 0 & \dots & 0 & 0 & 0 & \dots & 0 \\ 0 & 0 & \dots & 0 & 0 & 0 & \dots & 0 & 0 & 0 & \dots & 0 \end{bmatrix}$	$N_1 + N_2 + N_3 + 3$
Kirchhoff-Love	$\begin{bmatrix} 1 & X & \dots & X^{N_1} & 0 & 0 & \dots & 0 & 0 & 0 & \dots & 0 \\ 0 & 0 & \dots & 0 & 1 & X & \dots & X^{N_2} & 0 & 0 & \dots & 0 \\ 0 & 0 & \dots & 0 & 0 & 0 & \dots & 0 & 1 & X & \dots & X^{N_3} & 0 & 0 & \dots & 0 \\ 0 & 0 & \dots & 0 & 0 & 0 & \dots & 0 & 0 & 0 & \dots & 0 & 1 & X & \dots & X^{N_4} \\ 0 & 0 & \dots & 0 & 0 & 0 & \dots & 0 & 0 & 0 & \dots & 0 & 0 & 0 & \dots & 0 \\ 0 & 0 & \dots & 0 & 0 & 0 & \dots & 0 & 0 & 0 & \dots & 0 & 0 & 0 & \dots & 0 \end{bmatrix}$	$N_1 + N_2 + N_3 + N_4 + 4$

Table 3. Examples of base matrices of distributed joints (soft piece). N_1 , N_2 , N_3 , and N_4 are orders of polynomials used to fit the strains associated with different deformation modes. The generalized force ((τ_i)) of a distributed joint is given by,

$$\int_0^{L_i} \mathbf{B}_{\xi_i}^T \mathcal{F}_{a_i} dX_i$$

Name	Description
Bdof	6×1 array specifying the allowable DoFs of a soft piece: 1 if allowed 0 if not
Bodr	6×1 array specifying the order of allowed DoFs: (0 if constant, 1 if linear, 2 if quadratic,...)
B	Base matrix calculated at lumped joints or array of base matrices computed at every significant points of a soft piece
B_Z1, B_Z2	Base matrices calculated at points corresponding to the fourth order Zanna's collocation method
xi_starfn	Reference strain vector of the piece as a function of X
xi_star	6×1 reference strain vector at the lumped joint or column array of (6×3) matrices with reference strain vectors computed at Gauss quadrature and Zanna collocation points
dof	Total degrees of freedom of the piece

Table 4. Properties of Twist Class

Type	Name	Description
General Properties	N	Total number of links in series
	ntot	Total number of pieces
	ndof	Total degrees of freedom of linkage
	n_sig	Total number of points at which the computation is performed (significant points)
	VLinks	Vector of Link class elements of all links from the base to the tip of the linkage
	Vtwists	Vector of Twist class elements of all pieces from the base to the tip of the linkage
	Ltot	Total length of the linkage
	g_ini	Initial transformation matrix of the linkage (default value: $I(4)$)
	g0	Cell element of the initial transformation matrix of each piece
External Force Properties	q_scale	($ndof \times 1$) array of multipliers for each joint coordinate
	Gravity	Value is 1 if gravity is present, 0 if not
	G	Gravity wrench vector ($[0, 0, 0, g_x, g_y, g_z]^T$, where g is gravity vector)
	PointForce	Value is 1 if the linkage is subject to point force/moment, 0 if not
	np	Total number of point forces/moment
	Fp_loc	Cell element of piece numbers corresponding to the location of point forces/moment
	Fp_vec	Cell element of wrench vectors
	CEFP	Value is 1 if custom external force is present, 0 if not (default value: 0)
Actuation Properties	M_added	Added Mass (used for external force that depend on $\dot{\eta}$)
	Actuated	Value is 1 if the linkage is actuated, 0 if not
	nact	Total number of actuators
	Bqj1	Generalized actuation matrix of one dimensional joints
	n_jact	Total number of lumped joint actuators
	i_jact	Index of links who's joints are actuated
	i_jactq	Index of joint coordinates of all active joints
	Wrench-Controlled	($n_{jact} \times 1$) array of '1's' and '0's', where 1 indicates that the joint is controlled by wrench and 0 indicates that it is controlled by the joint coordinate(s).
	n_sact	Total number of soft link actuators
	dc	($n_{sact} \times N$) cell element of local cable positions $[0, y_p, z_p]^T$ at significant points of all active soft divisions
	dcp	Cell element of space derivatives of dc (with respect to x)
	Sdiv, Ediv	($n_{sact} \times N$) cell element of division numbers corresponding to the start and the end position of an actuator on a link
Elastic Properties	Inside	Value is 1 if the actuator is fully inside the linkage, 0 if not
	CAP	Value is 1 if custom actuation is present, 0 if not (default value: 0)
	CAS	Value is 1 for applying a custom actuator strength (default value: 0)
	K	Generalized stiffness matrix of the linkage
Elastic Properties	Damped	Value is 1 if the soft links are elastically damped 0 if not
	D	Generalized damping matrix of the linkage
	CP1, CP2, CP3	Constant custom properties of linkage

Table 5. Properties of Linkage Class

Name and syntax	Description
S.findg0	To get the initial transformation matrix of all pieces
S.FwdKinematics (q)	To get the transformation matrix at every significant points (arranged as column array)
S.Jacobian (q)	To get the Jacobian at every significant points (arranged as column array)
S.Jacobiandot (q, qd)	To get the derivative of Jacobian at every significant points (arranged as column array)
S.ScrewVelocity (q, qd)	To get the screw velocity at every significant points (arranged as column array)
S.findD	To compute and get the generalized damping matrix
S.findK	To compute and get the generalized stiffness matrix
S.ActuationMatrix (q)	To get the generalized actuation matrix (customized actuation is not included)
S.GeneralizedMassMatrix (q)	To get the generalized mass matrix
S.GeneralizedCoriolisMatrix (q, qd)	To get the generalized Coriolis matrix
S.GeneralizedExternalForce (q)	To get the generalized external force (customized external force is not included)
S.dynamics	For the dynamic simulation
S.statics	For the static equilibrium simulation
S.plotq0	To plot the free body diagram of the linkage
S.plotq (q)	To plot the state of the linkage for a given value of the joint coordinate
S.plotqqd (t, qqd)	To get dynamic simulation video output for a given t (time array) and qqd (array of joint coordinates and their time derivatives)

Table 6. Methods of the Linkage Class. S is the name of the Linkage.